

Efficient Privacy-Preserving Machine Learning with Lightweight Trusted Hardware

Pengzhi Huang Thang Hoang Yueying Li Elaine Shi G. Edward Suh
Cornell University Virginia Tech Cornell University Carnegie Mellon University Cornell University / Meta AI
ph448@cornell.edu thanghoang@vt.edu yl3469@cornell.edu runting@gmail.com edsuh@meta.com

Abstract—In this paper, we propose a new secure machine learning inference platform assisted by a small dedicated security processor, which will be easier to protect and deploy compared to today’s TEEs integrated into high-performance processors. Our platform provides three main advantages over the state-of-the-art: (i) We achieve significant performance improvements compared to state-of-the-art distributed Privacy-Preserving Machine Learning (PPML) protocols, with only a small security processor that is comparable to a discrete security chip such as the Trusted Platform Module (TPM) or on-chip security subsystems in SoCs similar to the Apple enclave processor. In the semi-honest setting with WAN/GPU, our scheme is $4\times$ - $63\times$ faster than Falcon (PoPETs’21) and AriaNN (PoPETs’22) and $3.8\times$ - $12\times$ more communication efficient. We achieve even higher performance improvements in the malicious setting. (ii) Our platform guarantees security with abort against malicious adversaries under honest majority assumption. (iii) Our technique is not limited by the size of secure memory in a TEE and can support high-capacity modern neural networks like ResNet18 and Transformer. While previous work investigated the use of high-performance TEEs in PPML, this work represents the first to show that even tiny secure hardware with really limited performance can be leveraged to significantly speed-up distributed PPML protocols if the protocol can be carefully designed for lightweight trusted hardware.

1. Introduction

As the world increasingly relies on machine learning for everyday tasks, a large amount of potentially sensitive or private data need to be processed by machine learning algorithms. For example, machine learning models for medical applications may need to use private datasets distributed in multiple nations as inputs [37]. A cloud-based machine learning services process private data from users with pre-trained models to provide predictions [1, 22]. The data to be shared in these applications are often private and sensitive and must be protected from the risk of leakage. Government regulations may play an essential role as a policy, but cannot guarantee actual protection. We need technical protection for privacy-preserving machine learning (PPML) for strong confidentiality and privacy guarantees.

In this paper, we propose a new PPML framework, named STAMP (Small Trusted hardware Assisted MPC), which enables far more efficient secure multiparty computation (MPC) for machine learning through a novel use of small lightweight trusted hardware (LTH). MPC refers to a protocol that allows multiple participants to jointly evaluate a particular problem while keeping their inputs from being revealed to each other. Ever since Yao’s initial studies (later called Garbled Circuit) [89, 90] which gave such a secure protocol in the case of two semi-honest parties, many studies have been conducted to improve the efficiency, to expand to more than two parties, and to ensure the feasibility against malicious behaviors. Recently, there has been significant interest in using and optimizing MPC for secure machine learning computation [54, 82, 83, 67, 40]. However, the overhead for MPC-based PPML is still significant.

For low-overhead secure computation, the trusted execution environments (TEEs) in modern microprocessors such as Intel SGX [12] AMD SEV [68] aim to provide hardware-based protection for the confidentiality and integrity of data and code inside. If the TEE protection and software inside can be trusted, secure machine learning computation can be performed directly inside a TEE with relatively low overhead [39]. The TEE can also be used to improve cryptographic protocols by accelerating bootstrapping [38, 48] or simplifying protocols [11, 2, 38, 18]. However, it is challenging to build a secure environment inside a high-performance processor due to its large trusted computing base (TCB) and complex performance optimizations such as out-of-order execution, speculation, and caching. For example, multiple attacks have been shown for SGX [79, 78, 23]. Moreover, the TEE requires adding hardware protection to each type of computing engines (CPU, GPU, and accelerators), and significant changes to the software stack. As a result, developing and deploying a TEE for a new piece of hardware requires significant effort and time.

In this paper, we propose to leverage a small dedicated security processor, another type of trusted hardware that is widely deployed today, to reduce the MPC overhead. For example, small discrete security chips such as trusted platform module (TPM), Google Titan, and Apple T1 are widely used to as a platform root-of-trust. Similarly, for system-on-chip (SoC) designs, on-chip security subsystems like the Apple enclave processor perform security-critical operations such

as secure booting, attestation, and key management¹.

While the high-level idea to combine trusted hardware and MPC has been explored before, we believe this work represents the first to investigate MPC acceleration using a small security processor. Clearly, such lightweight trusted hardware can only provide relatively low performance. The main question is if a low-performance trusted hardware can still be leveraged to provide meaningful speed-ups for MPC. In the following discussion, we refer to such small security processors as lightweight trusted hardware (LTH).

The key insight we leverage in STAMP is that non-linear operations, which can be performed very efficiently in plaintext, account for the major part of the overhead in MPC. MPC-based deep learning inference is not particularly expensive in computation but introduces large communication overhead due to multi-round data exchanges, especially when the network latency is high. This overhead leads to a very different cost distribution for MPC compared to plaintext computation. Profiling an inference task of AlexNet [42], which represents a classical deep learning model, shows that 85% of total plaintext execution time comes from linear operations such as convolution and fully-connected layers, while for MPC, this portion drops to only 5% with the remaining 95% coming from non-linear operations. Most of those non-linear operations are simple and cheap in plaintext (e.g., ReLU, MaxPooling, which are generally comparisons) with some exceptions (e.g., Softmax). This observation implies that even a lightweight trusted hardware can potentially speed up MPC-based PPML significantly if we can efficiently offload non-linear operations.

STAMP combines the advantages of MPC and trusted hardware by performing linear operations in MPC while leveraging LTH for non-linear operations. To realize this approach, we introduce new MPC protocols that efficiently offload non-linear operations while minimizing communications among multiple parties and between the LTH and an untrusted CPU/GPU. Although simple nonlinear operations can be performed inside the small LTH with sufficiently high performance, expensive operations such as Softmax require higher performance. To address the challenge, STAMP securely offloads parts of the expensive exponentiation operations. The following describes the main technical contributions and advantages of STAMP.

Overhead reduction. STAMP achieves significantly lower inference overhead compared to state-of-the-art MPC protocols with either CPU or GPU, under either a WAN or LAN setting. For various machine learning networks, the speedup can be $4\times$ to $63\times$, even with a tiny LTH with a low-bandwidth interconnect. Our analysis shows, as expected, the reduction of external network communication for non-linear functions significantly contributes to the speedup. We demonstrate that even with trust in a tiny piece of discrete

secure hardware similar to a TPM, significant speedups can be achieved for privacy-preserving neural network inference.

Malicious security. STAMP provides security guarantees under the honest-majority setting similar to previous schemes [83, 54], assuming that the majority (2 out of the 3 participants) are behaving honestly. If the corrupted party behaves semi-honestly, the protocol ensures that no information is obtained by any party without reconstructing a value. If a party is actively corrupted and behaves maliciously, we guarantee detection of such a behavior and output “abort” while still keeping the confidentiality of the data, with additional overhead compared to the semi-honest setting. We show the security of STAMP using the standard simulation-based paradigm in §B. We implement both semi-honest and malicious protocols in our end-to-end framework.

Evaluation and analysis. We implement STAMP in both CPU-only and GPU-assisted settings, and add the same GPU support to our baseline for a fair comparison. We demonstrate STAMP by supporting the secure inference of various networks including AlexNet [42], VGG16 [70], ResNet18 [28] and Transformer [86], over multiple datasets including MNIST [14], CIFAR-10 [41], ImageNet [66] and Wikitext-2 [50], under both WAN and LAN, and semi-honest and malicious settings. We provide theoretical analysis of the overhead and also perform detailed experimental studies. We therefore show that even a very small trusted hardware reduces the overhead of MPC protocols significantly while supporting various high-capacity networks.

Implementation and results. We implement the semi-honest and malicious protocols of STAMP using C++. The compilation framework and a small number of unchanged pure MPC-based operations (see §3.2 and §A) are based on [83]. The baseline framework was significantly modified to incorporate the new protocols for non-linear operations, support for GPUs, support for new networks and datasets, and a better socket library. The experimental results show that in a WAN / GPU setting, STAMP gains a $4\times$ to $63\times$ or $6\times$ to $59\times$ speed-up in semi-honest or malicious settings compared with the state-of-the-art protocols. The speed-ups with LAN and/or GPU are smaller, but STAMP still provides significantly performance improvement in all tests.

2. Model

In this section, we present our system model, threat model, and security model.

System Model. In our system, there are three parties who would like to run a common ML model together based on the input of individuals. We assume that the model structure is publicly known. We assume that each party consists of two components: an untrusted machine (CPU/GPU) and an LTH whose computational power is limited. We also assume that each party communicates with each other via a secure authenticated communication channel (e.g., SSL). LTH in each party communicates with each other through its host by establishing pairwise secure communication channels for data exchange.

1. These dedicated security chips and SoC subsystems are considered quite secure given that they are physically separated from the rest of the system and often also include more security features such as side-channel countermeasures. We envision our MPC extension can be realized as a firmware extension on today’s security processor.

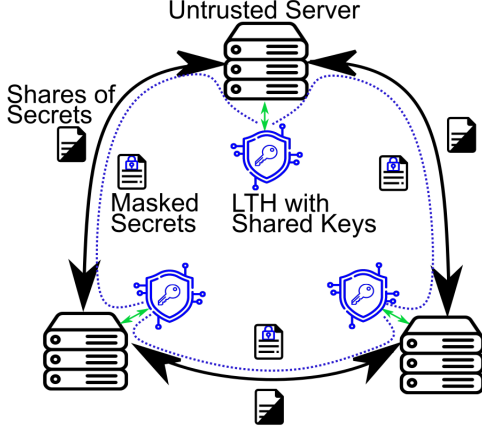


Figure 1: Diagram of participants and their communication channels. The black local machines owned by three parties, green local buses, and black inter-party communication channels are untrusted. The blue LTHs are trusted and contain blue keys shared among LTHs.

Threat Model. In our setting, we assume that a party or its server is untrusted except for the LTH. Specifically, we do not trust any of the server’s logic that includes a virtual machine monitor, an operating system, drivers, the software that manages storage, etc. We consider an honest majority, meaning that at most one party (except its LTH) can be malicious. The other two parties can be semi-honest, in which they may try to learn secrets (e.g., inputs or weights provided by other parties) while still following the protocol faithfully. The malicious adversary can deviate arbitrarily from the honest protocol, and its goal can be breaking the integrity of the evaluation by providing incorrect results without being noticed, or breaking the confidentiality of the data by learning the secrets. We assume that there is no collusion between any of the parties. We also assume that the confidentiality and the integrity of LTH cannot be compromised by an adversary to obtain data or alter its execution. That means there exists a Certificate Authority (CA) to validate the LTH during an initialization. Figure 1 provides an outline of STAMP, where the three LTHs act as three trusted third parties with established correlations (secret keys).

Security Model. In our system, the goal is to achieve the confidentiality and integrity of the ML model computation in the presence of a malicious adversary. We capture such confidentiality and integrity through simulation-based security [21, 7, 8] in the following definition.

Definition 1 (Simulation-based security: privacy and verifiability). A protocol $\pi_{\mathcal{F}}$ is said to securely realize the ideal functionality \mathcal{F} if for any probabilistic polynomial time (PPT) real-world adversary \mathcal{A} , there exists an ideal-world adversary \mathcal{S} such that for any PPT environment \mathcal{Z} , there exists a negligible function negl such that

$$|\Pr[\text{Real}_{\pi_{\mathcal{F}}, \mathcal{A}, \mathcal{Z}(\lambda)} = 1] - \Pr[\text{Ideal}_{\mathcal{F}, \mathcal{S}, \mathcal{Z}(\lambda)} = 1]| \leq \text{negl}(\lambda)$$

3. Background

In this section, we describe our notation, and then provide some prelims of MPC and trusted hardware.

3.1. Notation

We define L to be the finite field size, and \mathbb{Z}_L to be the finite field we are generally considering in this work. fp is the fix-point precision. We use the bold font \mathbf{a} or \mathbf{A} to represent a vector or a matrix. We use a_i , $(\mathbf{a})_i$ or $A_{i,j}$ to represent the i^{th} element of the vector \mathbf{a} or the element of the matrix \mathbf{A} in the i^{th} row and the j^{th} column. This is different from the bold \mathbf{A}_i , which still represents a matrix. Throughout the paper, if not specifically mentioned, all operations are carried out within the finite field \mathbb{Z}_L . When needed, we use $(a+b)_L$ to represent the modulo L operation for the output of the integer operations in brackets. We add a bar to a variable or operation, as \bar{a} , $\exp(\bar{a})$, to represent that a number or an output is a real number. The right-shift operation is indicated as \gg (e.g. $a \gg b = a/2^b$). We will often use two signed integers m, q to represent a positive real number \bar{a} as $\bar{a} = 2^q \cdot (m \gg 52) \in [0, 1)$, where m represents the mantissa part of 52 bits with $m \gg 52 \in [0, 1)$, and q_L is the exponent part. This is actually the format in which floating point numbers are represented following the IEEE Standard for Binary Floating-Point Arithmetic (IEEE 754-1985) [36], but without sign on the mantissa part. We use $\lfloor \bar{a} \rfloor$ to round a real number \bar{a} down to an integer.

3.2. Multiparty Computation

Notation. The sharing scheme we consider in this work is 2-out-of-3 replicated secret sharing scheme (RSS) modulo L . Let P_1, P_2, P_3 be the three parties participating in the evaluation. For convenience in notation, we use P_{i-1}, P_{i+1} to refer to the previous and next party of one party (e.g., the previous and the next party of P_1 are P_3 and P_2). The RSS of an integer secret $x \in \mathbb{Z}_L$ is denoted as $\llbracket x \rrbracket^L = (\llbracket x \rrbracket_1^L, \llbracket x \rrbracket_2^L, \llbracket x \rrbracket_3^L)$, where L is the size of the finite field to which the shares belong and $x = \llbracket x \rrbracket_1^L + \llbracket x \rrbracket_2^L + \llbracket x \rrbracket_3^L$. When we say that a secret x is shared as $\llbracket x \rrbracket^L$, it means that party P_i is holding $(\llbracket x \rrbracket_i^L, \llbracket x \rrbracket_{i+1}^L)$ for $i = 1, 2, 3$. To generate the integer representation x based on the real value \bar{x} , we use two’s complement fixed-point encoding with fp bits of precision. For a positive \bar{x} we have $x = \lfloor \bar{x} \cdot 2^{\text{fp}} \rfloor$, while for a negative \bar{x} , $x = \lfloor \bar{x} \cdot 2^{\text{fp}} \rfloor + L$, assuming that x is within the bound $[-L/2^{\text{fp}}, L/2^{\text{fp}}]$.

In our experiments, we mainly use the cases of $l = 32$, with $\text{fp} = 13$ and $L = 2^l$ (which supports inputs from -262144 to $262144 - 2^{-13}$), to match the bit-width used in the baseline MPC schemes. The security of a $l = 32$ setting naturally comes from the random masking creating the shares. Multiple existing MPC schemes [83, 67, 64, 10] use the 32-bit secret sharing setting and already prove its security. Our protocol and architecture can also use a larger field such as a 64-bit setting if a wider range of values need to be supported.

Multiplications are based on the protocols defined in [54, 82, 83, 13].

Multiplications. $\llbracket x \cdot y \rrbracket^L \leftarrow \Pi_{\text{Mul}}(\llbracket x \rrbracket^L, \llbracket y \rrbracket^L)$: To get $\llbracket z \rrbracket^L = \llbracket x \cdot y \rrbracket^L$, P_i would first compute $\hat{z}_i = \llbracket x_i \rrbracket^L \llbracket y_i \rrbracket^L + \llbracket x_{i+1} \rrbracket^L \llbracket y_i \rrbracket^L + \llbracket x_i \rrbracket^L \llbracket y_{i+1} \rrbracket^L$, then $(\hat{z}_1, \hat{z}_2, \hat{z}_3)$ is already a valid 3-out-of-3 secret sharing of xy since $z_1 + z_2 + z_3 = xy$. A reshare is needed to maintain the consistency of the 2-out-of-3 sharing scheme. To avoid any possible leakage of information, P_i uses the 3-out-of-3 randomness $\{\alpha_i\}$ to mask \hat{z}_i as $z_i = \hat{z}_i + \alpha_i$, then share it with P_{i-1} . Therefore, the parties obtain the necessary shares and $\llbracket z \rrbracket^L = \llbracket xy \rrbracket^L = (z_1, z_2, z_3)$ is built.

Matrix Multiplications. $\llbracket \mathbf{AB} \rrbracket^L \leftarrow \Pi_{\text{MatMul}}(\llbracket \mathbf{A} \rrbracket^L, \llbracket \mathbf{B} \rrbracket^L)$: To perform matrix multiplication $\llbracket \mathbf{C}_{a \times c} \rrbracket^L = \llbracket \mathbf{A}_{a \times b} \mathbf{B}_{b \times c} \rrbracket^L$, while simply applying Π_{Mul} for each multiplication leads to $\mathcal{O}(abc)$ shares to be sent, parties can instead perform matrix multiplication locally (i.e., $\llbracket \hat{\mathbf{C}} \rrbracket_i^L = \llbracket \mathbf{A} \rrbracket_i^L \llbracket \mathbf{B} \rrbracket_i^L + \llbracket \mathbf{A} \rrbracket_i^L \llbracket \mathbf{B} \rrbracket_{i+1}^L + \llbracket \mathbf{A} \rrbracket_{i+1}^L \llbracket \mathbf{B} \rrbracket_i^L$) and then share $\llbracket \hat{\mathbf{C}} \rrbracket_i^L$ at once. This strategy yields only $\mathcal{O}(ac)$ transmission overhead. As stated in [82], convolutions can be expanded into overall larger matrix multiplications.

The above protocols dealing with multiplications work well for integer representations, but will cause errors with fixed-point representations. A truncation protocol (right-shift the results by fp bits) must follow the multiplication to correct the fixed-point precision in 3-party MPC. We refer the readers to ABY3 [54] for more details on the 3-party truncation protocol, to prior work [54, 20] for details of the malicious variant of Π_{MatMul} , and to §A for other basic operations.

3.3. Trusted/Secure Hardware

Trusted/secure hardware has a long history of being successfully used in many high-security use cases, starting as dedicated security (co-)processors specializing in crypto operations. For example, smart cards [63] are widely used in financial transactions. Similarly, hardware security modules (HSMs) such as IBM 4758 [16] have also been used to protect critical secret keys. Discrete security chips such as TPM [60], Google Titan [31], and Apple T1 provide hardware root-of-trust on many platforms. Modern System-on-Chip (SoC) designs also typically include a dedicated security processor with crypto engines for secure booting and other high-security operations: Synopsys tRoot hardware security module [75], Rambus RT-630 programmable root-of-trust (RoT) [33], Apple secure enclave [30], Qualcomm secure processing unit [32], etc. These dedicated security processors usually require less than 1mm^2 . Even though their performance is limited and their implementations may still have security vulnerabilities [53, 26, 6], the small dedicated security processors are considered to be far more secure compared to high-performance processors as shown by their successful history in high-security applications. The dedicated security processors are also relatively easy to deploy as a separate chip or an IP block.

For high-performance processors, the idea of trusted hardware developed into a trusted execution environment

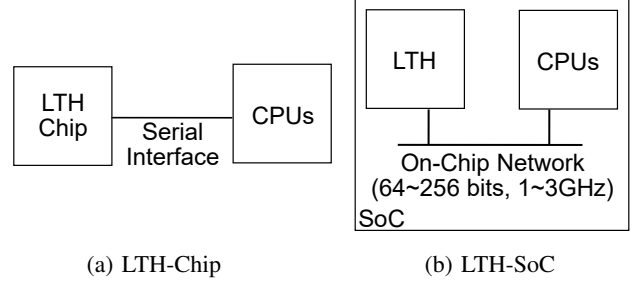


Figure 2: Two types of LTHs that STAMP considers.

(TEE), which adds hardware-based security protection on a shared general-purpose processor running a full software stack. A TEE aims to protect the integrity and confidentiality of the code and data inside, even when low-level software and/or the environment cannot be trusted. The TEE was first developed as a security extension on a high-performance processor such as Intel SGX [78] and recently also proposed for a secure accelerator [29].

While TEEs such as Intel SGX can directly run compute-intensive workloads such as machine learning, it is much more difficult to provide high security assurance or develop/deploy the high-performance TEEs compared to small dedicated security chips or SoC modules. A high-performance CPU contains millions of lines of code (LoCs) [44], takes hundreds of mm^2 in the silicon area, and is shared by many software components. Unfortunately, the large TCB and high complexity often lead to more vulnerabilities, as illustrated by many attacks found for high-performance TEEs, including page-fault-driven attacks [88, 69], segmentation-based attacks [25, 46], CPU cache-based attacks [23, 4], and enclave software attacks [45, 84]. In particular, the shared and general-purpose nature of a TEE requires protection from untrusted OS and side-channel attacks from co-located software, which dedicated security processors do not need to deal with. The high-performance TEE also requires new hardware protection for each computing engine and significant changes to a complex software stack, which makes its deployment for new hardware challenging.

In this work, we consider a lightweight trusted hardware (LTH) with performance and complexity similar to a traditional security chip or on-chip security subsystems in modern SoCs: a dedicated low-performance security processor that can support remote attestation to validate its identity and shared key exchanges (§4.1), has hardware crypto engines, and includes a programmable processor that can run code.

We consider two types of LTH designs as shown in Figure 2: 1) a discrete security chip similar to a TPM (LTH-chip), running at a low clock frequency (tens of MHz), and connected to a CPU through a low-bandwidth serial interface; and 2) a security subsystem module on an SoC (LTH-SoC), running at a much higher SoC clock frequency (1-3GHz), and connected to other processing engines (CPUs, GPUs, NPUs, etc.) on the same SoC through high-bandwidth on-chip networks. Our study suggests that even the discrete LTH-chip can significantly improve the

performance of MPC-based PPML.

Notation. Each party P_i is equipped with a LTH H_i , and H_i has a built-in PRF unit F (e.g., an AES engine) for pseudo-random number generation. We assume that even malicious participants cannot break the integrity and confidentiality guarantees that LTH provides. Details of the protocols executed in H_i will be introduced in §4.

3.4. Why LTH over High-Performance TEE?

While it is difficult to quantify the security, we believe that LTH provides strong security and deployment benefits over high-performance TEEs. As a reference, the survey of vulnerabilities of SGX and countermeasures [17] provides a good overview of the vulnerabilities in high-performance TEEs. Most vulnerability categories (address translation, CPU cache, DRAM, branch prediction, rowhammer) in the survey do not apply to LTH due to the following reasons:

Physical isolation: LTH is dedicated to a small set of security tasks, and physically separate from main processing cores with potentially malicious software. LTH tightly controls its software using secure booting and typically does not allow user software. Because hardware is not shared with potential attack software, there is much less concern for timing-channel attacks, which represent a main challenge in today’s TEEs.

Smaller TCB/attack surface, lower complexity: LTH uses a simple (in-order) processor with limited interfaces/commands for a small set of security tasks. Both hardware and software are much smaller and simpler compared to the main processors. Because there is no speculation or out-of-order execution, transient-execution attacks such as Meltdown/Spectre are not a concern for LTH. LTH does not have external memory (DRAM), and is not exposed to attacks on external memory such as DRAM probing and rowhammer attacks.

Side-channel protection: LTH such as smartcards, TPM, etc. are usually equipped with dedicated crypto engines and countermeasures (e.g., tamper-resistant circuits [73] for TPM, randomized block design [52] for smart cards) against physical side channels such as power side channels, while also having no off-chip memory to protect. In that sense, LTH is more robust against physical attacks.

Empirically, small dedicated security processors such as smartcards, TPM, Google Titan, Apple T1, and others have a long history of successfully being used in security-critical applications such as payments and cryptographic key management. The wide deployment of small security processors suggests that it is possible to make small dedicated hardware secure enough for many real-world applications.

Similar to how secure cryptographic primitives may be broken due to implementation-level vulnerabilities, LTH can still contain security vulnerabilities and may be compromised, especially through physical attacks. For example, timing side channels and power interrupts may make TPM private key recovery possible [53, 26]. Smart cards, although practically considered secure enough and well developed, have faced challenges including reverse engineering [61],

micro probing [71], optical fault induction attacks [72], and others. In that sense, the security guarantee of LTH is still not perfect and relies on secure hardware/software implementations under a certain threat model.

However, compared to complex high-performance TEEs, the vulnerabilities in LTH are far more limited and countermeasures against them are easier to apply in terms of cost and design complexity. In practice, the main security concerns for today’s TEE come from software-exploitable vulnerabilities. In that sense, LTH provides a major security benefit by removing most timing-channel or transient-execution vulnerabilities. While physical attacks are not considered a major threat in data-center environments, LTH can also provide strong physical security. LTH has no off-chip memory to protect, and often has anti-tamper/DPA countermeasures. On the other hand, recent TEEs target weaker threat models against physical attacks. Intel removed the integrity tree for replay protection in Icelake/TDX. AMD SEV has no replay protection against physical attacks. NVIDIA GPU TEE (H100) does not even encrypt its high-bandwidth memory (HBM).

4. The STAMP Protocol

This section introduces the details of the STAMP protocols in a semi-honest setting and the additional steps needed in a malicious setting.

4.1. Initialization phase

The initialization phase is a part of the offline phase (which needs no input data or model weights) of the protocol where the LTHs will have shared keys and initial values established in them if their identities are proven. Although Π_{init} plays an important role in our scheme, it is not where our main contribution lies, since mature remote attestation protocols already exist [3]. A proper remote attestation protocol is commonly supported in secure hardware such as a TPM [60], and validates the LTH’s identity and its state. This process can involve the acquisition of the certificate of a LTH from a trusted CA/Verifiers, which is usually the manufacturer of the it. H_i after being verified, can perform pairwise Diffie-Hellman key exchanges with a signature to obtain the shared key $k_{i-1,i}$ with H_{i-1} , $k_{i,i+1}$ with H_{i+1} , and then also $k_{i+1,i-1}$ through sharing masks. A simplified description of Π_{init} is shown in Protocol 1.

The communication out of H_i has to go through P_i , which provides a corrupted party with a natural way to observe or even alter the communication among the LTHs. For semi-honest adversaries, the Diffie-Hellman key exchange protocol already prevents them from obtaining the key with bounded computational resources. If the corrupted party behaves maliciously, Π_{init} does not have to take extra steps to detect such actions. If a malicious P_i modifies the remote attestation, a CA will not provide a certificate and P_i cannot create a certificate on its own, causing an abort. If a malicious P_i alters the transmission during key exchange, there will be no correct initialization established, and the

protocol will abort later when data inconsistency is detected later.

Protocol 1 Π_{Init} Initialization

Input. Security parameter λ .

Result. Output (Success, L) if the remote attestation succeeds and aborts if failed. After the initialization, LTHs (H_i) obtain shared keys and initial parameters.

- 1) Parties first agree to a L for the finite field \mathbb{Z}_L , size $l = \log L$ bits, prime p , and their order to define the previous and next party.
 - 2) P_i s perform remote attestation on each H_i to obtain a certificate from the CA and publicly share them to validate H_i . Abort if validation fails.
 - 3) H_i performs Diffie–Hellman key exchange with signature through the secure channel between P_i s to obtain $\mathcal{O}(\lambda)$ -bit PRF keys $k_{i,i+1}, k_{i-1,i}$, then use $F_{k_{i,i+1}}$ to mask one key $k'_{i-1,i} \equiv k_{i-1,i} + F_{k_{i,i+1}}(0) \pmod p$ and send $k'_{i-1,i}$ to H_{i+1} through P_i . H_i would receive $k'_{i+1,i-1}$ from H_{i-1} and can recover $k_{i+1,i-1} = k'_{i+1,i-1} - F_{k_{i+1,i-1}}(0)$.
-

The shared keys and the PRF in the LTHs can support the random number generation and are kept only known to the LTH, unlike the correlated randomness introduced in §A. With the shared keys in §4.1 and a built-in PRF F , we can now construct $\Pi_{\text{LTH.GenMask}}$ and $\Pi_{\text{LTH.GenMaskShare}}$ in the LTH as Protocol 2 and Protocol 3. They are very similar with only a minor difference that $\Pi_{\text{LTH.GenMaskShare}}$ always generates shares of 0. Four counters $\{\text{ctr}_1^i, \text{ctr}_2^i, \text{ctr}_3^i, \text{ctr}_s^i\}$ are used in each H_i to maintain consistency among H_i s in a semi-honest setting, and additional four $\{\hat{\text{ctr}}_1^i, \hat{\text{ctr}}_2^i, \hat{\text{ctr}}_3^i, \hat{\text{ctr}}_s^i\}$ are needed in a malicious setting for reduplicate execution for the detection of inconsistency. Notice that Protocol 2 and Protocol 3 gives the outputs to H_i , not P_i , and H_i may be set to give partial outputs in some protocols.

Protocol 2 $\mathbf{m} \leftarrow \Pi_{\text{LTH.GenMask}}(n, L, j; i, \text{ctr}_j^i, k_{j,j+1}^i)$

Input. The number of masks to be generated n , the index j for which counter, and which key to choose. The size of the finite field L , the counter ctr_j^i and the key $k_{j,j+1}^i$ are stored in the LTH.

Output. pseudo-random masks $\mathbf{m} \in \mathbb{Z}_L$ and updated counter ctr_j^i .

$\mathbf{m} = (F_{k_{j,j+1}^i}(\text{ctr}_j^i), F_{k_{j,j+1}^i}(\text{ctr}_j^i + 1), \dots, F_{k_{j,j+1}^i}(\text{ctr}_j^i + n - 1))$.
Update $\text{ctr}_j^i \leftarrow \text{ctr}_j^i + n$.

Protocol 3 $(\llbracket \mathbf{m}_j \rrbracket_i^L, \llbracket \mathbf{m}_j \rrbracket_{i+1}^L) \leftarrow \Pi_{\text{LTH.GenMaskShare}}(n, L; i, \text{ctr}_s^i, k_{i,i+1}^i, k_{i+1,i-1}^i, k_{i-1,i}^i)$

Input. The number of masks to be generated n . The size of the finite field L and the counter and keys are stored in the LTH.

Output. pseudorandom masks $\llbracket \mathbf{m} \rrbracket_i^L, \llbracket \mathbf{m} \rrbracket_{i+1}^L \in \mathbb{Z}_L$

$\llbracket m_j \rrbracket_i^L = F_{k_{i,i+1}^i}(\text{ctr}_s^i + j) - F_{k_{i+1,i-1}^i}(\text{ctr}_s^i + j)$ for $j = 0, \dots, n - 1$

$\llbracket m_j \rrbracket_{i+1}^L = F_{k_{i+1,i-1}^i}(\text{ctr}_s^i + j) - F_{k_{i-1,i}^i}(\text{ctr}_s^i + j)$ for $j = 0, \dots, n - 1$

Update $\text{ctr}_s^i \leftarrow \text{ctr}_s^i + n$.

4.2. ReLU

Non-linear layers used in a machine learning model are computationally light under plaintext. Π_{ReLU} , for exam-

ple, takes only one comparison and multiplexing. However, its complexity gets amplified significantly under the RSS scheme with more local computation steps and significant communication overhead (we will list and compare the theoretical complexities in §C). Now, aided by the LTH held by each party and the common randomness established in §4.1, we can significantly reduce the overhead by “offloading” the non-linear operations to the LTH. Although the LTH is far inferior in computation power compared to the untrusted machine, it can still remove much of the communication overhead in a pure MPC protocol.

In this section, we introduce Π_{ReLU} , the protocol to offload ReLU operations under MPC to trusted hardware. The steps we take are as follows: First, P_i invokes $\Pi_{\text{LTH.GenMask}}$ to get the pseudo-random masks, and sends $\llbracket x \rrbracket_i$ to P_{i+1} after adding them with the masks; Second, P_{i+1} adds the received value with the two shares it holds, then sends the results to the LTH; Third, H_{i+1} recovers the plaintext value by invoking $\Pi_{\text{LTH.GenMask}}$ using the same key and the counter with the same recorded number, and computes ReLU in plaintext, re-masks the result with $\Pi_{\text{LTH.GenMaskShare}}$, and sends them back to P_{i+1} . The other two parties will also generate their common share in the meantime; Fourth, P_{i+1} re-shares the received values to complete the construction of the RSS of the outputs.

Π_{ReLU} is given in Protocol 4 for the semi-honest setting in black. The extra steps marked in blue are only executed when malicious security is needed, and we use this notation in other protocols as well. The malicious version generally adds replicate parallel operations and requires replicate sharing of the same values to validate the integrity. Parties compare the copies of intermediate results and final outputs from different sources to achieve malicious security with abort.

After the protocol, $\{\text{ctr}_{1,2}^i, \text{ctr}_{2,3}^i, \text{ctr}_{3,1}^i, \text{ctr}_s^i\}$ for $i = 1, 2, 3$ all increase by n , and $\{\hat{\text{ctr}}_{1,2}^i, \hat{\text{ctr}}_{2,3}^i, \hat{\text{ctr}}_{3,1}^i, \hat{\text{ctr}}_s^i\}$ for $i = 1, 2, 3$ all increase by n too in a malicious setting. The synchronization of the counters together with shared keys guarantees the correlated randomness among the LTHs.

One may notice that the workload is not balanced among the three parties if we fix i . In the protocol, the party index i can be any of $\{1, 2, 3\}$, which means that the three parties can start the protocol simultaneously with a disjoint dataset. Therefore, when provided with a batch B of inputs for evaluation, each party can work on the $B/3$ data and start the corresponding protocol simultaneously, balancing resource usage and reducing overall latency.

4.3. Further Optimization of ReLU

As introduced in §3.2, in a fixed-point setting, truncation is required after each multiplication to keep the consistency of the precision. We also observe that for classical networks [42, 86, 70, 28], the layers containing matrix multiplications such as convolution (Conv) and fully-connected (FC) layers are often applying ReLU to the results at the end. If we apply Protocol 4 directly after the completion of multiplications, the communication overhead will be the multiplication

Protocol 4 $\llbracket \text{ReLU}(\mathbf{x}) \rrbracket^L \leftarrow \Pi_{\text{ReLU}}(\llbracket \mathbf{x} \rrbracket^L)$ Do ReLU on shares of vector \mathbf{x}

Input. Each $\{P_i\}$ owns $\llbracket \mathbf{x} \rrbracket^L$.

Output. Each $\{P_i\}$ gets $\llbracket \mathbf{z} \rrbracket^L = \llbracket \text{ReLU}(\mathbf{x}) \rrbracket^L$.

- 1) P_i calls H_i to execute $\Pi_{\text{LTH.GenMask}}(n, L, i - 1)$ to obtain the masks $\mathbf{m}_{i-1} \in \mathbb{Z}_L^n$ then compute $\mathbf{x}'_{i-1} = \llbracket \mathbf{x} \rrbracket^L_{i-1} + \mathbf{m}_{i-1}$.
Malicious: P_{i-1} generates $\mathbf{m}_{i-1} = \Pi_{\text{LTH.GenMask}}(n, L, i - 1)$ and $\mathbf{x}'_{i-1} = \llbracket \mathbf{x} \rrbracket^L_{i-1} + \mathbf{m}_{i-1}$, and P_{i-1}, P_{i+1} also generates $\mathbf{m}_{i+1} = \Pi_{\text{LTH.GenMask}}(n, L, i + 1)$, $\mathbf{x}'_{i+1} = \llbracket \mathbf{x} \rrbracket^L_{i+1} + \mathbf{m}_{i+1}$.
 - 2) P_i send \mathbf{x}'_{i-1} to P_{i+1} .
Malicious: P_{i-1} send \mathbf{x}'_{i-1} to P_{i+1} ; P_{i-1} and P_{i+1} send \mathbf{x}'_{i+1} to P_i .
 - 3) P_{i+1} , after receiving \mathbf{x}'_{i-1} add it to $\llbracket \mathbf{x} \rrbracket^L_i, \llbracket \mathbf{x} \rrbracket^L_{i+1}$ and pass it to H_{i+1} .
Malicious: P_i, P_{i+1} check the two copies received and abort if any inconsistency is found. P_i execute as above with index $i - 1$ replacing index i .
 - 4) **LTH Only** : H_{i+1} recovers the plaintext $\mathbf{x} = (\mathbf{x}'_{i-1} + \llbracket \mathbf{x} \rrbracket^L_i + \llbracket \mathbf{x} \rrbracket^L_{i+1}) - \mathbf{m}_{i-1}$ where \mathbf{m}_{i-1} is generated with $\Pi_{\text{LTH.GenMask}}(n, L, i - 1)$. Set $\mathbf{b} = (\mathbf{x} > \mathbf{0})$. Then H_{i+1} invokes $\Pi_{\text{LTH.GenMaskShare}}(n, L)$ to get $\llbracket \mathbf{z}^* \rrbracket^L_i, \llbracket \mathbf{z}^* \rrbracket^L_{i+1} \in \mathbb{Z}_L^n$, and compute: $(\llbracket z_j \rrbracket^L_i, \llbracket z_j \rrbracket^L_{i+1}) = ((b_j ? x_j : 0) + \llbracket z_j^* \rrbracket^L_i, \llbracket z_j^* \rrbracket^L_{i+1})$. Return their values to P_{i+1} .
 H_i and H_{i-1} invokes $\Pi_{\text{LTH.GenMaskShare}}(n, L)$ to get $\llbracket \mathbf{z} \rrbracket^L_{i-1} \in \mathbb{Z}_L^n$, and invokes $\Pi_{\text{LTH.GenMaskShare}}(n, 2)$ to get $\llbracket \mathbf{b} \rrbracket^L_{i-1} \in \mathbb{Z}_2^n$. Return them respectively to P_i and P_{i-1} .
Malicious: H_i perform the same step as above with index $i - 1$ replacing index i , replacing $\Pi_{\text{LTH.GenMaskShare}}$ with $\Pi'_{\text{LTH.GenMaskShare}}$, while also masking the results with the masks of index i (i.e., $(\llbracket z_j \rrbracket^L_{i-1}, \llbracket z_j \rrbracket^L_i) = (\llbracket z_j^* \rrbracket^L_{i-1}, (b_j ? x_j : 0) + \llbracket z_j^* \rrbracket^L_i)$). H_{i-1} and H_{i+1} generate the remaining share $\llbracket z_j \rrbracket^L_{i+1}$ for P_{i-1} and P_{i+1} respectively.
 - 5) P_{i+1} send $\llbracket \mathbf{z} \rrbracket^L_i$ to P_i , send $\llbracket \mathbf{z} \rrbracket^L_{i+1}$ to P_{i-1} . Now $\llbracket \mathbf{z} \rrbracket^L$ and $\llbracket \mathbf{b} \rrbracket^L$ are calculated and shared to each party.
Malicious: P_i shares to P_{i-1} and P_{i+1} respectively. Each party checks the copies they receive and aborts if an inconsistency is found.
-

/ truncation overhead and the Protocol 4 overhead summed, which is not optimal. Since truncation itself is also a simple non-linear function in plaintext (which is just right-shift), we can exploit this common structure in deep learning models and merge the truncation with the following non-linear operations to be simply computed together in plaintext inside the trusted LTH.

The protocol $\Pi_{\text{MatMulReLU}}$ showing how ReLU can be combined with truncation after matrix multiplication is given in Protocol 5. Extra communication has to be done compared to Protocol 4, because the parties hold 3-out-of-3 sharing instead of 2-out-of-3 after local steps of multiplication, as described in §3.2. $\Pi_{\text{MatMulReLU}}$ reduces the total communication rounds of matrix multiplication and ReLU combined to 2 from at least 3, and also saves the total amount of data to be transmitted by merging the step 2) of Protocol 4 with the communication needed during truncation. For the malicious setting, we use $\Pi_{\text{mal-arith-mult}}$ of [54] to ensure correct 2-out-of-3 shares after local multiplication, then make the replicate execution as we did in Protocol 4.

4.4. Extensions to Other Operations

The protocols mentioned in §4.2 can be extended to common non-linear operations needed in deep learning networks, including $\Pi_{\text{MaxPooling}}, \Pi_{\text{BatchNorm}}, \Pi_{\text{LayerNorm}}$. $\Pi_{\text{MaxPooling}}$ only needs comparisons and multiplexing. $\Pi_{\text{BatchNorm}}$ and $\Pi_{\text{LayerNorm}}$ need about two multiplications for each element on average. Their low complexity allows them to be offloaded to the LTH in a similar way as Π_{ReLU} . Minor changes are needed in step 4) of Π_{ReLU} . $\Pi_{\text{MatMulReLU}}$ can be extended to others in a similar way, changing step 5) of $\Pi_{\text{MatMulReLU}}$. To optimize neural networks in our experiments, we also use $\Pi_{\text{MatMulMaxPoolReLU}}$,

$\Pi_{\text{MatMulBatchNormReLU}}$, constructed with minor changes in step 5) of Π_{ReLU} .

4.5. Softmax

Exponentiation is an essential component of modern deep learning models. For example, logistic or softmax requires exponentiation. In this work, we focus on softmax, which is extensively used in modern models such as Transformers [86]. The way classical MPC [40, 62] realizes softmax leads to a large overhead due to two main reasons: 1. the complex protocol to approximate the exponentiation; 2. the max function to be applied before softmax. A recent study [85] shows that softmax is the main source of overhead when running a Transformer network with an MPC protocol and also introduces a numerical stability problem.

The Softmax on a vector \mathbf{x} is defined as follows:

$$\text{Softmax}(\mathbf{x}) := \exp(\mathbf{x}) / \sum_{i=1}^n \exp(\mathbf{x}_i) \quad (1)$$

In a regular ML setting, taking exponentiation over a value can easily lead to overflow, especially in a fixed-point representation, which MPC protocols need to use. The traditional solution to the overflow issue is to take the maximum of the input \mathbf{x} and then subtract it from every element before feeding it into the softmax function. The risk of overflowing is removed as the maximum input value would be 0. However, the extra max operation introduces an even more considerable overhead to an MPC protocol, as shown in the recent study [85].

A naïve extension of the previous protocol for exp would be to move exp to the LTH, similar to the other non-linear operations in §4.2. This would not work due to the low computational power of the LTH and the large amount of computation needed for exp compared to other operations.

Protocol 5 $[\text{ReLU}(\mathbf{A} \times \mathbf{B})]^L \leftarrow \Pi_{\text{MatMulReLU}}([\mathbf{A}]^L, [\mathbf{B}])$: Multiply \mathbf{A} and \mathbf{B} , then output the shares of the ReLU of the results.

Input. $\{P_i\}$ have shares of $\mathbf{A} \in \mathbf{Z}_L^{a \times b}$ and $\mathbf{B} \in \mathbf{Z}_L^{b \times c}$.

Output. $\{P_i\}$ get shares of $[\mathbf{Z}]^L = [\text{ReLU}(\mathbf{A} \times \mathbf{B})]^L$.

- 1) P_1, P_2 , and P_3 locally computes $[\hat{\mathbf{C}}]_i^L = [\mathbf{A}]_i^L \times [\mathbf{B}]_i^L + [\mathbf{A}]_i^L \times [\mathbf{B}]_{i+1}^L + [\mathbf{A}]_{i+1}^L \times [\mathbf{B}]_i^L$.
Malicious: Parties instead perform $\Pi_{\text{mal-arith-mult}}$ of [54] to ensure that the multiplications (before truncation) were performed faithfully by parties. In the end, the 2-out-of-3 sharing $[\hat{\mathbf{C}}]$ is distributed.
 - 2) P_i calls H_i to execute $\Pi_{\text{LTH.GenMaskShare}}(a \times c, L)$ to obtain the masks $[\mathbf{M}]_i \in \mathbf{Z}_L^{a \times c}$, then compute $\hat{\mathbf{C}}'_i = [\hat{\mathbf{C}}]_i^L + [\mathbf{M}]_i$. P_{i-1} also calls H_{i-1} to perform $\Pi_{\text{LTH.GenMaskShare}}(a \times c, L)$ to obtain $[\mathbf{M}]_{i-1} \in \mathbf{Z}_L^{a \times c}$ and $\hat{\mathbf{C}}'_{i-1} = [\hat{\mathbf{C}}]_{i-1}^L + [\mathbf{M}]_{i-1}$.
Malicious: Instead of doing the semi-honest protocol, P_{i+1}, P_{i-1} generates $[\mathbf{M}]_{i+1} \leftarrow \Pi_{\text{LTH.GenMask}}(a \times c, L, i+1)$ and $\hat{\mathbf{C}}'_{i+1} = [\hat{\mathbf{C}}]_{i+1}^L + [\mathbf{M}]_{i+1}$. P_{i-1}, P_i also generates $[\mathbf{M}]_{i-1}$ invoking $\Pi'_{\text{LTH.GenMask}}(a \times c, L, i-1)$, $\hat{\mathbf{C}}'_{i-1} = [\hat{\mathbf{C}}]_{i-1}^L + [\mathbf{M}]_{i-1}$.
 - 3) P_i and P_{i-1} send $\hat{\mathbf{C}}'_i$ and $\hat{\mathbf{C}}'_{i-1}$ to P_{i+1} .
Malicious: Instead of doing the semi-honest protocol, P_{i+1}, P_{i-1} send $\hat{\mathbf{C}}'_{i+1}$ to P_i ; P_{i-1}, P_i send $\hat{\mathbf{C}}'_{i-1}$ to P_{i+1} .
 - 4) P_{i+1} computes $\hat{\mathbf{C}}' = \hat{\mathbf{C}}'_i + \hat{\mathbf{C}}'_{i-1} + [\hat{\mathbf{C}}]_{i+1}^L$ and passes it to H_{i+1} .
Malicious: Instead of doing the semi-honest protocol, P_i, P_{i+1} compare the two received copies and abort if inconsistency is found. P_i computes $\hat{\mathbf{C}}' = \hat{\mathbf{C}}'_{i+1} + [\hat{\mathbf{C}}]_{i-1}^L + [\hat{\mathbf{C}}]_i^L$ and passes it to H_i , P_{i+1} computes $\hat{\mathbf{C}}' = \hat{\mathbf{C}}'_{i-1} + [\hat{\mathbf{C}}]_i^L + [\hat{\mathbf{C}}]_{i+1}^L$ and passes it to H_{i+1} .
 - 5) **LTH Only** : H_{i+1} generates the masks $[\mathbf{M}]_{i+1}$ by invoking $\Pi_{\text{LTH.GenMaskShare}}(a \times c, L)$ and recovers the plaintext through truncation: $\hat{\mathbf{C}} = \lfloor (\hat{\mathbf{C}}' + [\mathbf{M}]_{i+1}) \gg \text{fp} \rfloor$. Note that $[\mathbf{M}]_{i+1} + [\mathbf{M}]_i + [\mathbf{M}]_{i-1} = \mathbf{0}$.
Set $\mathbf{D} = (\hat{\mathbf{C}} > \mathbf{0})$. Then H_{i+1} invokes $\Pi_{\text{LTH.GenMaskShare}}(a \times c, L)$ to get $[\mathbf{Z}^*]_i^L \in \mathbf{Z}_L^{a \times c}$, $[\mathbf{Z}^*]_{i+1}^L \in \mathbf{Z}_L^{a \times c}$, and compute:
 $([\mathbf{Z}_{j,k}]_i^L, [\mathbf{Z}_{j,k}]_{i+1}^L) = ((D_{j,k} ? C_{j,k} : 0) + [\mathbf{Z}^*_{j,k}]_i^L, [\mathbf{Z}^*_{j,k}]_{i+1}^L)$. Return them to P_{i+1} .
 P_i and P_{i-1} call H_i and H_{i-1} to invoke $\Pi_{\text{LTH.GenMaskShare}}(a \times c, L)$ to get $[\mathbf{Z}]_{i-1}^L \in \mathbf{Z}_L^{a \times c}$.
Malicious: Instead, H_{i+1} generates masks with $\Pi_{\text{LTH.GenMask}}(a \times c, L, i-1)$ to recover the plaintext
 $\hat{\mathbf{C}} = \lfloor (\hat{\mathbf{C}}' - [\mathbf{M}]_{i-1}) \gg \text{fp} \rfloor$, with the remaining being the same. H_i do as above respectively with index i replacing index $i+1$, replacing $\Pi_{\text{LTH.GenMask}}$ with $\Pi'_{\text{LTH.GenMask}}$, and fix that the plaintext results are added to mask share i . $\Pi_{\text{LTH.GenMaskShare}}(a \times c, L)$ is invoked at last to generate the shares. H_{i-1} also generates the remaining share for P_{i-1} .
 - 6) P_{i+1} send $[\mathbf{Z}]_i^L, [\mathbf{D}]_i^L$ to P_i , send $[\mathbf{Z}]_{i+1}^L, [\mathbf{D}]_{i+1}^L$ to P_{i-1} . Now, $[\mathbf{Z}]^L$ and $[\mathbf{D}]^L$ are calculated and shared with each party.
Malicious: P_i shares $[\mathbf{Z}]_{i-1}^L, [\mathbf{D}]_{i-1}^L$ and $[\mathbf{Z}]_i^L, [\mathbf{D}]_i^L$ to P_{i-1} and P_{i+1} respectively. Each party checks the results from the parallel two computations and aborts if an inconsistency is found.
-

Under our assumption on the trusted hardware (details in §5), tests show that 1 million 32-bit multiplications take less than a second, while double-precision exponentiation takes over a minute. Unlike simple non-linear operations, exp needs to be done with floating point arithmetic for high precision, and each exp can involve tens of multiplications during the process. This approach will lead to significant overhead on a small LTH, and introduce a new bottleneck for our scheme.

Our solution is to split and “offload” the computation to the untrusted local machine. The most complex part of the exp operation is performed by the powerful but untrusted CPU/GPU, and then the results are assembled within the LTH. The main idea of the protocol is based on the fact that $\exp(a + b + c) = \exp(a) \exp(b) \exp(c)$, which implies that untrusted machines can complete exp on individual shares so that only simple multiplications are done inside of the LTH. However, challenges remain to keep the protocol secure while also dealing with the conversion between fixed-point representations and real-number arithmetic. In Protocol 6, we expand the exponent part (see §3.1) to contain all possible results of $\exp(\lfloor x \rfloor_i^L)$, specifically for $L = 2^{32}$. Overflow would not occur in our protocol after this adjustment, even without invoking max function before Softmax.

4.6. Security analysis

We claim the following three theorems hold:

Theorem 1. Under the assumption of secure PRF and LTH, Π_{ReLU} (in Protocol 4) securely realizes the ideal functionality $\mathcal{F}_{\text{ReLU}}$ (in Figure 5) against any non-uniform PPT malicious adversary that can corrupt up to 1 out of 3 parties with static corruption.

Theorem 2. Under the assumption of secure PRF and LTH, $\Pi_{\text{MatMulReLU}}$ (in Protocol 5) securely realizes the ideal functionality $\mathcal{F}_{\text{MatMulReLU}}$ against any non-uniform PPT malicious adversary that can corrupt up to 1 out of 3 parties with static corruption.

Theorem 3. Under the assumption of secure PRF and LTH, Π_{Softmax} (in Protocol 6) securely realizes the ideal functionality $\mathcal{F}_{\text{Softmax}}$ against any non-uniform PPT malicious adversary that can corrupt up to 1 out of 3 parties with static corruption.

Due to space limitations, we refer the reader to §B for formal proofs of Theorem 1 under corrupted P_1 , and how the proof can be extended to other corrupted party choices and the other two theorems.

5. Evaluation

5.1. Experimental Setup

Implementation and baselines. We implemented STAMP in C++. Our implementation is based on Falcon [83], keeping the basic MPC protocols, adding the new protocols, adding GPU supports for linear layers, and switching

Protocol 6 $\Pi_{\text{Softmax}}(\mathbf{x})$ compute softmax

Input. $\{P_i\}$ have replicative shares of $\mathbf{x} \in \mathbb{Z}_L^n$.

Output. $\{P_i\}$ get $\llbracket \exp(\mathbf{x}) \rrbracket^L$

Initial values. The LTHs save (q_L, m_L) for later use where $2^{q_L} \cdot (m_L \gg 52) = \exp(L \gg \text{fp})$, $q_L \in \mathbb{Z}_{2^{32}}$, $m_L \in \mathbb{Z}_{2^{52}}$, $(m_L \gg 52) \in [0, 1)$. fp is the fixed-point precision. We note $\bar{\mathbf{x}}$ to be the real values that \mathbf{x} represents.

- 1) For each $\llbracket x_j \rrbracket^L$, P_i computes $\bar{r} = \frac{\exp(\llbracket x_j \rrbracket_{i-1}^L \gg \text{fp})}{\exp(\llbracket x_j \rrbracket_{i-1}^L \gg \text{fp})}$. Let $\bar{r} = \frac{\exp(\llbracket x_j \rrbracket_{i-1}^L \gg \text{fp})}{\exp(\llbracket x_j \rrbracket_{i-1}^L \gg \text{fp})} = 2^{q_j} \cdot (m_j \gg 52)$ where m_j has no sign since it is always positive. ($q_j = \lfloor \log_2(\exp(\llbracket x_j \rrbracket_{i-1}^L \gg \text{fp})) \rfloor = \lfloor \log_2(\llbracket x_j \rrbracket_{i-1}^L \gg \text{fp}) \cdot \log_2(e) \rfloor < 2^{32}$. We can see that 32 bits are enough to store q_j).
Invoke $\Pi_{\text{LTH.GenMask}}$ from H_i to generate two masks $\alpha_j \in \mathbb{Z}_{2^{52}}$ and $\beta_j \in \mathbb{Z}_{2^{32}}$ for $j = 1, \dots, n$ with the corresponding dimension (use truncation to match the dimensions), and send $\{m_j^* = (m_j + \alpha_j)_{2^{52}}, q_j^* = (q_j + \beta_j)_{2^{32}}\}$ for $i = 1, \dots, n$ to P_{i+1} .
Malicious: P_{i-1} follows the same computation to get $\{m_j^*, q_j^*\}$ to P_{i+1} . P_{i-1}, P_{i+1} additionally compute $\bar{r} = \frac{\exp(\llbracket x_j \rrbracket_{i+1}^L \gg \text{fp})}{\exp(\llbracket x_j \rrbracket_{i+1}^L \gg \text{fp})}$ and obtain $\{m_j^*, q_j^*\}$ by masking the mantissa and exponent part with masks from $\Pi_{\text{LTH.GenMask}}$, send them to P_i .
- 2) P_{i+1} receives $\{q_j^*, m_j^*\}$ and computes $2^{q_j} \cdot \hat{m}_j := \frac{\exp(\llbracket x_j \rrbracket_{i+1}^L + \llbracket x_j \rrbracket_i^L \gg \text{fp})}{\exp(\llbracket x_j \rrbracket_{i+1}^L + \llbracket x_j \rrbracket_i^L \gg \text{fp})}$. Send $\{\mathbf{q}^* + \hat{\mathbf{q}}, \mathbf{m}^*, \hat{\mathbf{m}}\}$ to H_{i+1} .
Malicious: P_{i+1} and P_i compare the two received copies and abort if an inconsistency is found. P_i do the same computation as above with index i replacing index $i - 1$, and send the obtained $\{\mathbf{q}^* + \hat{\mathbf{q}}, \mathbf{m}^*, \hat{\mathbf{m}}\}$ to H_i .
- 3) **LTH Only:** H_{i+1} Generate α_j and β_j , Compute $q_j' = (q_j^* + \hat{q}_j) - \beta_j = q_j + \hat{q}_j$, $m_j' = (m_j^* - \alpha_j) \cdot \hat{m}_j = m_j \cdot \hat{m}_j$. Define the results $2^{q_j'} \cdot m_j' := \frac{\exp(\llbracket x_j \rrbracket_i^L \gg \text{fp}) \cdot \exp(\llbracket x_j \rrbracket_{i-1}^L + \llbracket x_j \rrbracket_{i+1}^L \gg \text{fp})}{\exp(\llbracket x_j \rrbracket_{i-1}^L + \llbracket x_j \rrbracket_{i+1}^L + \llbracket x_j \rrbracket_i^L \gg \text{fp})}$.
For the fixed-point representation $x_j \in [0, L)$, the real value it represents $\bar{x}_j \in [-L/2 \gg \text{fp}, L/2 \gg \text{fp})$, $\lfloor \log_2(\exp(x_j)) \rfloor \in [-L/2 \gg \text{fp} \cdot \log_2(e), (L/2) \gg \text{fp} \cdot \log_2(e)]$. Set the q -bound: $\mathbf{qb} = ((L/2) \gg \text{fp}) \cdot \log_2(e)$. Define $\exp(\bar{x}_j) := 2^{q_j'} \cdot (m_j' \gg 52)$, then q_j'' should be in $[-\mathbf{qb}, \mathbf{qb}]$.
 q_j' and m_j' may alter from the correct q_j'' and m_j'' for two possible reasons: We are missing an L to be subtracted if $(\llbracket x_j \rrbracket_{i-1}^L + \llbracket x_j \rrbracket_{i+1}^L)_L + \llbracket x_j \rrbracket_i^L \neq (\llbracket x_j \rrbracket_i^L + \llbracket x_j \rrbracket_{i+1}^L + \llbracket x_j \rrbracket_{i-1}^L)_L = x_j$; or \bar{x}_j , or the real value x_j represents is actually negative, so $\bar{x}_j = ((\llbracket x_j \rrbracket_i^L + \llbracket x_j \rrbracket_{i+1}^L + \llbracket x_j \rrbracket_{i-1}^L)_L - L) \gg \text{fp}$. H_{i+1} runs:
 - a) If $q_j' \in (0, \mathbf{qb}]$, $q_j'' = q_j'$, $m_j'' = m_j'$.
 - b) If $q_j' \in (\mathbf{qb}, 3 * \mathbf{qb}]$, we are missing one $\exp(-L \gg \text{fp})$ to be multiplied for either reason. Compute $q_j'' = q_j' - q_L$, $m_j'' = (m_j^* - \alpha_j) \cdot \hat{m}_j / m_L$.
 - c) If $q_j' \in (3 * \mathbf{qb}, 5 * \mathbf{qb}]$, we are missing $\exp(-2L \gg \text{fp})$ to be multiplied for both reasons. Compute $q_j'' = q_j' - 2 * q_L$, $m_j'' = (m_j^* - \alpha_j) \cdot \hat{m}_j / (m_L)^2$.

Now H_{i+1} obtains the corrected $\exp(\bar{x}_j) = 2^{q_j''} (m_j'' \gg 52)$. H_{i+1} then compute softmax of the real values directly by $\text{Softmax}(\bar{\mathbf{x}}) = \exp(\bar{\mathbf{x}}) / \sum(\exp(\bar{\mathbf{x}}))$ which involves only $\mathcal{O}(n)$ additions, $\mathcal{O}(1)$ multiplications and divisions. Then convert the results to fixed-point representations, and invoke $\Pi_{\text{LTH.GenMaskShare}}$ for masks $\llbracket \mathbf{m} \rrbracket_{i+1}^L, \llbracket \mathbf{m} \rrbracket_i^L$ to output

$(\llbracket \mathbf{y} \rrbracket_i^L, \llbracket \mathbf{y} \rrbracket_{i+1}^L) = (\text{Softmax}(\mathbf{x}) + \llbracket \mathbf{m} \rrbracket_i^L, \llbracket \mathbf{m} \rrbracket_{i+1}^L)$ to P_{i+1} .

P_i and P_{i-1} call H_i and H_{i-1} to generate $\llbracket \mathbf{m} \rrbracket_i^L = \Pi_{\text{LTH.GenMaskShare}}(n)$ as $(\llbracket \mathbf{y} \rrbracket_{i-1}^L)$.

Malicious: H_i do the computation accordingly, while also masking the results with the index masks i . P_{i-1} call H_{i-1} to generate $(\llbracket \mathbf{m} \rrbracket_{i+1}^L, \llbracket \mathbf{m} \rrbracket_{i-1}^L) = \Pi_{\text{LTH.GenMaskShare}}(n, L)$ as $(\llbracket \mathbf{y} \rrbracket_{i+1}^L, \llbracket \mathbf{y} \rrbracket_{i-1}^L)$.

- 4) P_{i+1} share $\llbracket \mathbf{y} \rrbracket_i^L$ with P_i and $\llbracket \mathbf{y} \rrbracket_{i+1}^L$ with P_{i-1} .
Malicious: P_i shares $\llbracket \mathbf{y} \rrbracket_{i-1}^L$ to P_{i-1} and $\llbracket \mathbf{y} \rrbracket_i^L$ to P_{i+1} respectively. Each party checks the results of the two parallel computations and aborts if an inconsistency is found.
-

the networking library to ZeroMQ. Falcon is the main framework we compare to, but the open-source project was not implemented to support GPUs and does not address a key protocol for Transformers: Softmax. As a baseline, we extended Falcon and called this new baseline Falcon+, which includes three improvements over Falcon: 1. GPU support for linear layers, 2. a new MPC protocol for π_{softmax} , which is implemented using the exponentiation protocol of [40] combined with Π_{Div} and Π_{Max} provided by Falcon, 3. ZeroMQ [91] as a networking library for better performance and fair comparison with the proposed scheme. These changes do not affect the threat model.

We also compare our scheme with AriaNN [67], but we use Falcon as the primary baseline for a few reasons. We found that Falcon and AriaNN are comparable; AriaNN shows benefits compared to Falcon in some settings, but also disadvantages in others before our optimizations for Falcon+. AriaNN consumes a large amount of memory due to its technique, e.g., a server with 64GB DRAM can only

support inputs of batch size 8 for ResNet18 inference, while 32GB is enough for batch size 128 in our case.

Hardware and network. We run our experiments on Cloudlab c240g5 machines over Ubuntu 20.04 LTS with an Intel Xeon Silver 4114 10-core CPU at 2.20 GHz and a NVIDIA 12GB P100 GPU. Our network setup is similar to previous studies [83, 82, 67, 55]; the LAN has 625 MBps bandwidth and around 0.2 ms ping time, and the WAN has 40 MBps bandwidth and 70 ms ping time. Both semi-honest and malicious settings are tested. For the LTH-chip, we use Arduino Due with Atmel SAM3X8E ARM Cortex-M3 CPU (84MHz, 512 KB of Flash and up to 100 KB of SRAM), which is used for a commercial TPM implementation [77], to evaluate the LTH runtime. We also assume that the LTH has the low-pin-count (LPC) bus (same as a TPM), which leads to a 15MBps bandwidth limit in our experiments. The capability of a TPM to generate random numbers will not meet our need for throughput. As shown in [74], a maximum of 3MBps of generation can be achieved in a TPM, which is

enough for its original use case, but not for our scheme. We assume that a low-cost hardware AES engine [15] is added, and its throughput of 14 GBps makes the LTH’s pseudo-random number generation time negligible compared to the data transmission time through the low bandwidth interconnect. Other details of the hardware can be seen in §5.4. For the LTH-SoC, we assume the same Cortex-M3 processor running at 1GHz and the 128-bit on-chip network (16GBps). The performance is estimated by scaling the execution time of the discrete LTH.

Neural networks and Dataset. We use 8 neural networks: a small 3-layer fully-connected network with ReLU activations (Network-A, as in SecureML [55]), a small convolutional network with ReLU activation (Network-B, as in [64]), a small convolutional network with ReLU activation and maxpooling (Network-C, as in [47]), AlexNet [42], VGG16 [70], ResNet18 [28] and a small Transformer [80]. We pick the small Transformer network with limited dimensions and a small number of multi-head attention due to the fact that Softmax is too expensive in pure MPC for a reasonable evaluation time, especially in a WAN setting. The input data sets are MNIST [14] for the first four networks, CIFAR-10 [41] for AlexNet and VGG16, ImageNet [66] for ResNet18, and Wikitext-2 [50] for the Transformer.

Parameter choice. As mentioned in §4.5, we choose $L = 2^{32}$ and $\text{fp} = 13$ in our implementation. We pick the group size to be 2048 bits in Diffie–Hellman key exchange and use AES-128 for the pseudo-random number generation.

5.2. Performance

Table 1 and Table 2 show the end-to-end latency (in seconds) of the inference on inputs of batch size 128 in semi-honest and malicious settings, respectively. Table 3 and Table 4 report the amount of data transmitted. ‘-’ in the cells indicates that the implementation is missing or the network is too large for CPU evaluation. AriaNN does not implement its work in a malicious setting.

In the tables, we compare STAMP with Falcon [83] and AriaNN [67], two of the state-of-the-art MPC frameworks. AriaNN does not implement the execution of different parties on separate machines, but instead uses the local simulation of the network for performance evaluation. Depending on the structure of the machine learning network, STAMP with LTH-chip is $4\times$ to $63\times$ or $6\times$ to $59\times$ faster than the state-of-the-art MPC results with semi-honest or malicious settings in WAN / GPU environments. The advantage that we obtain under a LAN or CPU environment is smaller compared to a WAN/GPU environment. In the LAN, communication overhead is significantly reduced. With a CPU, the computation accounts for a larger portion of the execution time. These factors reduce the speedup, which is mainly accomplished by reducing the communication overhead of non-linear functions. STAMP with LTH-SoC achieves even higher speedup because LTH-SoC has higher performance compared to LTH-chip thanks to its higher clock frequency and the data movement between an LTH and a CPU/GPU is also faster on an SoC. The performance

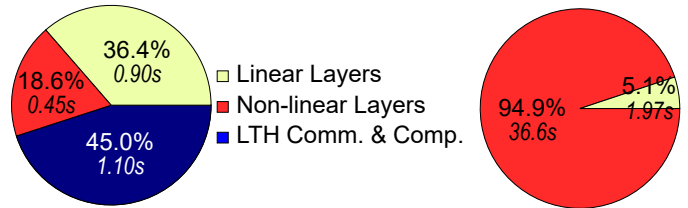


Figure 3: The breakdown of local machine execution time: linear layers, non-linear layers, and LTH-Chip bus communication & computation time. STAMP (left) and Falcon+ (right) on semi-honest inference over AlexNet under WAN/GPU.

gap between LTH-SoC and LTH-chip is the largest in LAN / GPU environments where local communication overhead is large. Also, note that for smaller networks, a GPU can be slower than a CPU. For a small amount of data and a small deep learning model, initialization and data movement may take more time than operating directly on a CPU.

In Figure 3, we show the time breakdown of semi-honest inference over AlexNet under the WAN/GPU setting. In both STAMP and Falcon+, linear layers take a similar amount of time. However, they contribute only 5.1% of the total execution time in Falcon+, and over 36% in STAMP, because the non-linear layers’ runtime is significantly reduced from about 94.9% to 18.6% (63.6% if we roughly consider all operations on the LTH are related to non-linear layers. There is some overhead, such as the local transmission in step 4 of Protocol 5, which cannot be assigned to be only linear or non-linear operations). Table 5 shows another breakdown of the execution time in the WAN/GPU setting: CPU/GPU, communication, and LTH. Note that we are moving major parts of the computation of most non-linear operations to the LTH, so the CPU/GPU execution time is also reduced.

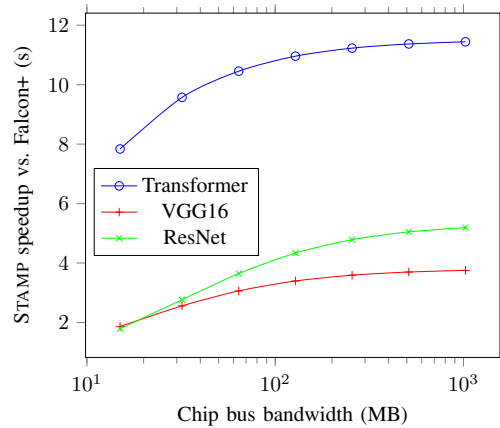


Figure 4: The speedup with different bus bandwidth in the semi-honest setting under LAN/GPU.

STAMP trades off the inter-party communication with the local communication between LTH and the untrusted CPU/GPU. However, as can be seen in Table 3 and Table 4, for LTH-chip, the low (15 MBps) bus bandwidth becomes

Table 1: Inference time (s) of a 128 batch in a semi-honest setting. AriaNN has a reduced batch size of 64 and 8 for VGG16 and ResNet18 due to memory consumption, which also applies to other tables.

Framework	Network-A				Network-B				Network-C			
	LAN GPU	LAN CPU	WAN GPU	WAN CPU	LAN GPU	LAN CPU	WAN GPU	WAN CPU	LAN GPU	LAN CPU	WAN GPU	WAN CPU
Falcon+	0.0824	0.1118	1.478	1.393	0.2034	0.2618	1.464	1.292	1.866	2.191	7.321	7.288
AriaNN	0.2560	0.5120	-	5.504	-	-	-	-	3.072	5.248	-	17.02
STAMP-chip speed-up	0.0737	0.0777	0.2516	0.2946	0.1172	0.1142	0.2787	0.2938	0.6809	1.298	1.024	1.494
STAMP-SoC speed-up	1.11×	1.43×	5.87×	4.72×	1.73×	2.29×	5.25×	4.39×	2.74×	1.68×	7.14×	4.87×
STAMP-SoC speed-up	0.0432	0.0472	0.2211	0.2641	0.0643	0.0613	0.1994	0.2408	0.1990	0.8163	0.5424	1.012
	1.91×	2.37×	6.69×	5.28×	3.17×	4.28×	7.34×	5.37×	9.38×	3.10×	13.5×	7.20×
Framework	LeNet				AlexNet				Transformer			
	LAN GPU	LAN CPU	WAN GPU	WAN CPU	LAN GPU	LAN CPU	WAN GPU	WAN CPU	LAN GPU	LAN CPU	WAN GPU	WAN CPU
Falcon+	2.592	4.603	8.867	9.563	4.276	11.78	38.56	43.06	4.026	-	321.0	-
AriaNN	4.480	7.040	-	18.30	9.984	19.20	-	43.52	-	-	-	-
STAMP-chip speed-up	0.9693	3.075	1.315	3.255	1.564	9.263	2.463	9.449	0.5130	-	5.024	-
STAMP-SoC speed-up	2.67×	1.49×	6.74×	2.93×	2.73×	1.27×	15.6×	4.55×	7.84×	-	63.8×	-
STAMP-SoC speed-up	0.2869	2.392	0.6328	2.573	0.3055	8.029	1.229	8.215	0.3618	-	4.873	-
	9.04×	2.02×	14.0×	3.72×	14.0×	1.52×	31.3×	5.24×	11.1×	-	65.8×	-
Framework	VGG16				ResNet18							
	LAN GPU	LAN CPU	WAN GPU	WAN CPU	LAN GPU	LAN CPU	WAN GPU	WAN CPU				
Falcon+	49.36	-	122.1	-	545.9	-	1439	-				
AriaNN*	198.4	-	-	-	1779	-	-	-				
STAMP-chip speed-up	26.55	-	30.05	-	309.7	-	350.7	-				
STAMP-SoC speed-up	1.85×	-	4.06×	-	1.76×	-	4.10×	-				
STAMP-SoC speed-up	13.06	-	16.56	-	106.9	-	148.0	-				
	3.78×	-	7.37×	-	5.10×	-	9.72×	-				

a bottleneck of our performance with large networks, especially in the LAN setting. In Table 3, almost 3GB of data is transmitted through the LTH-CPU bus for the ResNet18 reference, causing more than 200 seconds of communication time, which is about 60% of the total execution time of our scheme. LTH-SoC provides much higher LTH-CPU bandwidth and significantly alleviate this bottleneck.

Figure 4 shows how the speedup over Falcon+ can change if we use a higher-bandwidth interconnect for the LTH. In this figure, we choose two computation-heavy networks, VGG16 and ResNet18, and a communication-heavy Transformer network (due to frequently used Softmax) as examples. We can observe a considerable boost in performance with a higher LTH bandwidth.

Pure CPU TEE Solution. We also obtain the results achieved by a pure TEE solution as a reference. The pure SGX experiment assumes that semi-honest parties can securely share their data to one party’s SGX for evaluation and is executed on SGX V1 with 16GB enclave memory on Azure Standard DC4s v3. For smaller networks such as Network-B, SGX performs slightly worse, 0.46 seconds compared to 0.12 of STAMP, mostly due to the initialization overhead. For larger networks such as ResNet18, however, Intel SGX only takes 8.15 seconds, while STAMP (LTH-SoC) takes 148 second. This is expected since the TEE-only solution has no inter-party communication, as its drawbacks are discussed in §3.3. The complete table is shown in §D.

5.3. Accuracy

The precision of the inference using the plaintext computation and model weights is shown in Table 6, where the model weights are from the plaintext training. For Network-A, B, C and LeNet, which are measured by Falcon [83], STAMP has the same accuracy that Falcon achieved. STAMP optimizes overhead, but does not change computation precision with the same L and fp . In most schemes, for each batch of 128 elements, only one more sample would be classified incorrectly compared with the plaintext results, mainly due to the quantization when converting data from floating-point precision to fixed-point precision. However if some weights and activations are outside of the fix-point representation range, the inference accuracy may degrade more significantly. Carefully capping the values during plaintext training can potentially help avoiding this issue.

5.4. Hardware Overhead of LTH

The LTH in STAMP consists of two parts:

- 1) The core microcontroller with the same capability as a TPM. We refer to the design of ST33TPM12SPI as a baseline with 0.40mm^2 area for the ARM SecurCore SC300. The detailed parameters can be found on the product page [77]. It will be responsible for most protocols with a peak power consumption of 12mW .
- 2) An AES engine performing pseudo-random number generation. A previous study [15] reports a cost of 0.13mm^2 and 56mW in area and peak power con-

Table 2: Inference time (s) of a 128 batch in a malicious setting. AriaNN does not implement their work in a malicious setting.

Framework	Network-A				Network-B				Network-C			
	LAN GPU	LAN CPU	WAN GPU	WAN CPU	LAN GPU	LAN CPU	WAN GPU	WAN CPU	LAN GPU	LAN CPU	WAN GPU	WAN CPU
Falcon+	0.1921	0.3293	3.359	3.3701	0.6279	0.6416	3.504	3.0743	5.639	6.758	23.26	20.8988
STAMP-chip	0.0913	0.2567	0.5150	0.7307	0.1594	0.2860	0.5803	0.7246	1.157	3.661	2.196	4.258
speed-up	2.10×	1.51×	6.52×	4.61×	3.94×	2.82×	6.04×	4.24×	4.87×	2.12×	10.6×	4.91×
STAMP-SoC	0.0200	0.1854	0.4437	0.6594	0.0357	0.1623	0.4566	0.6010	0.0325	2.536	1.071	3.134
speed-up	9.59×	2.09×	7.57×	5.11×	17.5×	4.98×	7.67×	5.12×	173×	3.06×	21.7×	6.67×
Framework	LeNet				AlexNet				Transformer			
	LAN GPU	LAN CPU	WAN GPU	WAN CPU	LAN GPU	LAN CPU	WAN GPU	WAN CPU	LAN GPU	LAN CPU	WAN GPU	WAN CPU
Falcon+	7.492	15.38	28.82	32.57	13.89	41.88	100.9	123.2	10.99	-	777.9	-
STAMP-chip	2.106	10.64	2.929	10.80	3.653	36.80	5.538	36.10	2.073	-	13.03	-
speed-up	3.56×	1.55×	9.84×	3.01×	3.80×	1.27×	18.2×	3.41×	5.30×	-	59.6×	-
STAMP-SoC	0.5136	9.052	1.337	9.213	0.7738	33.92	2.659	33.22	1.720	-	12.68	-
speed-up	14.5×	1.82×	21.5×	3.54×	17.9×	1.37×	37.9×	3.71×	6.39×	-	61.3×	-
Framework	VGG16				ResNet18							
	LAN GPU	LAN CPU	WAN GPU	WAN CPU	LAN GPU	LAN CPU	WAN GPU	WAN CPU				
Falcon+	136.9	-	407.8	-	1550	-	4993	-				
STAMP-chip	51.54	-	68.09	-	639.3	-	772.2	-				
speed-up	2.66×	-	5.99×	-	2.43×	-	6.47×	-				
STAMP-SoC	20.06	-	36.62	-	166.2	-	299.1	-				
speed-up	6.82×	-	11.1×	-	9.33×	-	16.6×	-				

Table 3: Inference communication(MB) of a 128 batch in a semi-honest setting.

Framework	Network-A	Network-B	Network-C	LeNet	AlexNet	Transformer	VGG16	ResNet18	
Falcon+	Inter-party	1.536	6.272	64.87	95.33	173.5	72.21	1730	22933
AriaNN	Inter-party	2.816	-	38.54	55.04	121.6	-	1161	18944
STAMP	Inter-party	0.2058	0.8371	5.328	7.931	12.31	19.21	187.7	2106
	LTH-CPU	0.4585	0.7958	7.235	10.24	18.53	2.270	202.5	3044

Table 4: Inference communication (MB) of a 128 batch in a malicious setting.

Framework	Network-A	Network-B	Network-C	LeNet	AlexNet	Transformer	VGG16	ResNet18	
Falcon+	Inter-party	10.51	41.33	423.4	620.1	1135	340.0	11543	139287
STAMP	Inter-party	0.8443	2.0704	21.02	28.80	48.68	131.2	838.6	7500
	LTH-CPU	1.070	1.856	16.88	23.90	43.23	5.296	472.5	7103

Table 5: Inference time (s) breakdown of a 128 batch in a semi-honest WAN/GPU setting, comparing with Falcon+.

Framework	Component	Network-A		Network-B		Network-C		LeNet		AlexNet		Transformer		VGG16		ResNet18	
		Time	Ratio	Time	Ratio	Time	Ratio	Time	Ratio	Time	Ratio	Time	Ratio	Time	Ratio	Time	Ratio
STAMP	CPU/GPU	0.04	17%	0.06	23%	0.19	19%	0.28	21%	0.29	12%	0.30	6%	12.8	43%	98.0	28%
	Comm.	0.18	70%	0.16	58%	0.35	34%	0.35	27%	0.94	38%	4.56	91%	3.34	11%	44.0	13%
	LTH	0.03	13%	0.05	19%	0.48	47%	0.68	52%	1.24	50%	0.16	3%	13.8	46%	207	59%
Falcon+	CPU/GPU	0.08	6%	0.20	14%	1.80	25%	2.50	28%	4.09	11%	3.95	1%	47.6	39%	523	36%
	Comm.	1.40	94%	1.27	86%	5.52	75%	6.37	72%	34.4	89%	317	99%	74.4	61%	916	64%

Table 6: Accuracy on different networks. The weights of ResNet18 are from Torchvision [49].

Network	Plaintext Accuracy	STAMP Accuracy
Network-A	98.18%	97.42%
Network-B	98.93%	97.81%
Network-C	99.16%	98.64%
LeNet	99.76%	99.15%
ResNet18@1	84.76%	84.37%
ResNet18@5	95.80%	95.50%

sumption. The AES engine serves as the PRF F in $\Pi_{LTH.GenMask}$ and $\Pi_{LTH.GenMaskShare}$.

The combined overhead of $0.53mm^2$ and $68mW$ is quite small, suggesting that LTH is cheaper and easier to deploy compared to adding a TEE to a high-performance processor. LTH may even be implemented as a simple extension of the existing TPM hardware or the on-chip SoC security subsystem. Furthermore, our protocol can be deployed with existing or future hardware platforms without integrating new TEE features directly into them. We note that the LTH overhead here does not represent the full power consumption of STAMP, which also need to run an MPC protocol on an untrusted CPU/GPU.

5.5. Trusted Computing Base (TCB)

As the security of a system is difficult to quantify, the TCB size is often used as a proxy when comparing system designs. Our estimates suggest that LTH has a much smaller TCB compared to a high-performance TEE. For the hardware TCB, open-source microcontrollers whose complexity is comparable to LTH that we use have $<20k$ Lines-of-Code (LoC) (OpenRISC: 16k LoC + AES: 1k LoC). While the LoC for commercial TEE hardware is not publicly available, the area of high-performance processors (Intel Skylake: $322mm^2 \sim 698mm^2$, Intel Sapphire Rapids: $\sim 400mm^2$) is much larger than the size of LTH ($0.53mm^2$).

For the software TCB, our LTH software implementation has $\sim 13k$ LoC. On the other hand, the software TCB for the Intel SGX experiment includes Gramine ($\sim 50k$ LoC) and PyTorch ($\sim 166k$ LoC) inside a TEE. For, virtual machine (VM) based TEEs such as Intel TDX and AMD SEV the software TCB can be much larger as the entire operating system (OS), drivers, and ML software stack (PyTorch) all need to run inside a TEE (millions of LoC for Linux).

6. Related Work

Encrypted computation (MPC/HE) for machine learning. Cryptographic techniques such as garbled circuits [9, 65], secret sharing [67, 54, 82], homomorphic encryption [55, 92] have been applied for privacy-preserving inference. Gazelle and Delphi [35, 51] combine homomorphic encryption and garbled circuits for their advantages in linear and non-linear operations, respectively. Falcon [83] implements a 3-party malicious secure protocol, combining techniques from SecureNN [82] and ABY3 [54]. Blaze [59] achieves not only 3-party malicious security but also fairness in an honest majority setting. AriaNN [67] leverages function secret sharing to reduce communication rounds for specific functions, but at the cost of increasing the total amount of communication data in some cases. CrypTen [40] provides a general software framework that makes secure MPC primitives more easily used by integrating them into a popular ML framework, PyTorch. GForce [56] proposed fusing layers in MPC, and more specifically combined dequantization and quantization layers into a truncation before and after ReLU and MaxPooling. Our protocol also applies layer fusing when applicable, but in the context of reducing overhead for non-linear operations in LTH. Our work leverages the recent developments in MPC for PPML, but shows that a simple security processor can significantly reduce the high overhead of today’s MPC-based PPML methods.

Combination of trusted hardware and crypto-based secure computation. Recent studies explored multiple approaches to improve MPC/HE for machine learning using trusted hardware. However, the previous work typically assumes a high-performance TEE such as Intel SGX and relies on the TEE to perform a significant amount of computation, which will be too slow on a small security processor. To the best of our knowledge, our work is the first to show that even a small low-performance security processor can significantly

improve the performance of MPC if the protocol can be carefully designed for lightweight trusted hardware.

For performance improvements, the previous studied proposed using a TEE (Intel SGX) to accelerate bootstrapping [38, 48], perform faster functional encryption [19], and simplify certain protocols [11, 38, 18]. The previous work also investigated splitting the work between a TEE (Intel SGX) and MPC. For example, Gupta et al. [24] propose splitting secure computation between garbled circuits and Intel SGX. Zhou et al. [93] introduce a two-party TEE-aided MPC scheme that focuses on improving multiplication overhead by moving part of the linear operations to a TEE. HYBRTC [87] decides where the computation should be run based on whether or not the parties trust a TEE; a hybrid protocol moves the computation to the TEE or just performs an MPC protocol. While the high-level approach of offloading computation from MPC to trusted hardware is similar, the previous work offloaded heavy computation to a high-performance TEE while our work studies how to leverage a low-performance security processor.

Slalom [76] and Darknight [27] propose to run a private machine learning computation on an untrusted GPU by securely outsourcing linear operations from the CPU TEE (SGX) to the GPU using secret sharing, and later Goten [57] proposed an improved scheme compared with Slalom by introducing “dynamic quantization” for training. While the use of pseudorandom masks is similar to our protocol in Slalom, Slalom uses masking only for outsourcing linear operations, as the other two papers. As a result, non-linear operations cannot be offloaded, and the CPU TEE still needs to perform as many linear operations as a GPU in an offline phase. These approaches require a high-performance TEE, and the TEE performance limits the overall secure computation performance. STAMP, on the other hand, only requires small low-performance trusted hardware for non-linear operations by performing linear operations on untrusted CPUs/GPUs using MPC. Also, Slalom utilizes its pseudorandom masks with the pure additive linear homomorphism of functions. Our approach of computing Softmax has a similar idea but involves multiplicative homomorphism as shown in §4.5.

Trusted hardware can also be used to improve the security of an MPC protocol. For example, CryptFlow [43] runs MPC protocols on Intel SGX and leverages SGX’s integrity protection to achieve malicious security. Another work [5] uses Intel SGX to protect the data of parties in MPC even if they are remotely hacked.

Trusted hardware-based privacy-preserving machine learning. The previous work investigated performing and optimizing machine learning computation inside a CPU TEE (Intel SGX) [39], and providing stronger side-channel protection through data-oblivious computation [58]. The performance of a TEE can be further improved by introducing the TEE capabilities to GPUs [81, 34] and domain-specific accelerators [29]. While the TEE on a high-performance CPU/GPU/accelerator is capable of providing much higher performance compared to MPC-based machine learning computation, the approach comes with the challenges in securing complex high-performance hardware as well as

the cost of developing and deploying new hardware and software. STAMP is the first to combine a small security processor with MPC for privacy-preserving machine learning, introducing a new trade-off point between security and performance.

7. Conclusion

This paper introduces a new PPML system which significantly reduces the overhead of MPC with the assistance of an LTH. STAMP can guarantee security against malicious corrupted parties in an honest-majority 3-party setting. Theoretical analysis and experimental results show that STAMP achieves orders of magnitude higher performance over state-of-the-art MPC protocols in various environments, even with an LTH whose performance is comparable to a TPM.

References

- [1] *Azure Machine Learning Studio*. <https://azure.microsoft.com/en-us/services/machine-learning/>.
- [2] Raad Bahmani et al. “Secure multiparty computation from SGX”. In: *International Conference on Financial Cryptography and Data Security*. Springer. 2017, pp. 477–497.
- [3] Alexander Sprogø Banks, Marek Kisiel, and Philip Korsholm. “Remote attestation: a literature review”. In: *arXiv preprint arXiv:2105.02466* (2021).
- [4] Ferdinand Brasser et al. “Software grand exposure: SGX cache attacks are practical”. In: *11th USENIX Workshop on Offensive Technologies (WOOT 17)*. 2017.
- [5] Brandon Broadnax et al. “Fortified Multi-Party Computation: Taking Advantage of Simple Secure Hardware Modules”. In: *Proceedings on Privacy Enhancing Technologies 2021.4* (2021), pp. 312–338.
- [6] John Butterworth et al. “Bios chronomancy: Fixing the core root of trust for measurement”. In: *Proceedings of the 2013 ACM SIGSAC conference on Computer & Communications Security*. 2013, pp. 25–36.
- [7] Ran Canetti. “Security and composition of multiparty cryptographic protocols”. In: *Journal of CRYPTOLOGY* 13.1 (2000), pp. 143–202.
- [8] Ran Canetti. “Universally composable security: A new paradigm for cryptographic protocols”. In: *Proceedings 42nd IEEE Symposium on Foundations of Computer Science*. IEEE. 2001, pp. 136–145.
- [9] Nishanth Chandran et al. “EzPC: programmable, efficient, and scalable secure two-party computation for machine learning”. In: *Cryptology ePrint Archive* (2017).
- [10] Harsh Chaudhari et al. “Astra: High throughput 3pc over rings with application to secure prediction”. In: *Proceedings of the 2019 ACM SIGSAC Conference on Cloud Computing Security Workshop*. 2019, pp. 81–92.
- [11] Joseph I Choi et al. “A hybrid approach to secure function evaluation using SGX”. In: *Proceedings of the 2019 ACM Asia Conference on Computer and Communications Security*. 2019, pp. 100–113.
- [12] Victor Costan and Srinivas Devadas. “Intel SGX explained”. In: *Cryptology ePrint Archive* (2016).
- [13] Daniel Demmler, Thomas Schneider, and Michael Zohner. “ABY-A framework for efficient mixed-protocol secure two-party computation.” In: *NDSS*. 2015.
- [14] Li Deng. “The mnist database of handwritten digit images for machine learning research”. In: *IEEE Signal Processing Magazine* 29.6 (2012), pp. 141–142.
- [15] Pham-Khoi Dong, Hung K Nguyen, and Xuan-Tu Tran. “A 45nm high-throughput and low latency aes encryption for real-time applications”. In: *2019 19th International Symposium on Communications and Information Technologies (ISCIT)*. IEEE. 2019, pp. 196–200.
- [16] Joan G Dyer et al. “Building the IBM 4758 secure coprocessor”. In: *Computer* 34.10 (2001), pp. 57–66.
- [17] Shufan Fei et al. “Security vulnerabilities of SGX and countermeasures: A survey”. In: *ACM Computing Surveys (CSUR)* 54.6 (2021), pp. 1–36.
- [18] Susanne Felsen et al. “Secure and private function evaluation with Intel SGX”. In: *Proceedings of the 2019 ACM SIGSAC Conference on Cloud Computing Security Workshop*. 2019, pp. 165–181.
- [19] Ben Fisch et al. “Iron: functional encryption using Intel SGX”. In: *Proceedings of the 2017 ACM SIGSAC Conference on Computer and Communications Security*. 2017, pp. 765–782.
- [20] Jun Furukawa et al. “High-throughput secure three-party computation for malicious adversaries and an honest majority”. In: *Annual international conference on the theory and applications of cryptographic techniques*. Springer. 2017, pp. 225–255.
- [21] Oded Goldreich, Silvio Micali, and Avi Wigderson. “How to play any mental game, or a completeness theorem for protocols with honest majority”. In: *Providing Sound Foundations for Cryptography: On the Work of Shafi Goldwasser and Silvio Micali*. 2019, pp. 307–328.
- [22] *Google Cloud AI*. <https://cloud.google.com/products/machine-learning/>.
- [23] Johannes Götzfried et al. “Cache attacks on Intel SGX”. In: *Proceedings of the 10th European Workshop on Systems Security*. 2017, pp. 1–6.
- [24] Debayan Gupta et al. “Using intel software guard extensions for efficient two-party secure function evaluation”. In: *International Conference on Financial Cryptography and Data Security*. Springer. 2016, pp. 302–318.
- [25] Jago Gyselinck et al. “Off-limits: Abusing legacy x86 memory segmentation to spy on enclaved execution”. In: *International Symposium on Engineering Secure Software and Systems*. Springer. 2018, pp. 44–60.
- [26] Seunghun Han et al. “A bad dream: Subverting trusted platform module while you are sleeping”. In: *27th {USENIX} Security Symposium ({USENIX} Security 18)*. 2018, pp. 1229–1246.
- [27] Hanieh Hashemi, Yongqin Wang, and Murali Annavaram. “Darknight: A data privacy scheme for training and inference of deep neural networks”. In: *arXiv preprint arXiv:2006.01300* (2020).
- [28] Kaiming He et al. “Deep residual learning for image recognition”. In: *Proceedings of the IEEE conference on computer vision and pattern recognition*. 2016, pp. 770–778.
- [29] Weizhe Hua et al. “Guardnn: Secure dnn accelerator for privacy-preserving deep learning”. In: *arXiv preprint arXiv:2008.11632* (2020).
- [30] Apple Inc. *Apple Secure Enclave*. URL: <https://support.apple.com/guide/security/secure-enclave-sec59b0b31ff/web> (visited on 10/03/2022).
- [31] Google Inc. *Google Titan Key*. URL: <https://cloud.google.com/titan-security-key/> (visited on 10/03/2022).

- [32] Qualcomm Incorporated. *Qualcomm Secure Processing Unit*. URL: <https://www.qualcomm.com/news/releases/2019/06/qualcomm-snapdragon-855-becomes-first-mobile-soc-receive-smart-card> (visited on 10/03/2022).
- [33] Rambus Incorporated. *RT-630 Programmable Root of Trust*. URL: <https://www.rambus.com/security/root-of-trust/rt-630/> (visited on 10/03/2022).
- [34] Insu Jang et al. “Heterogeneous isolated execution for commodity gpus”. In: *Proceedings of the Twenty-Fourth International Conference on Architectural Support for Programming Languages and Operating Systems*. 2019, pp. 455–468.
- [35] Chiraag Juvekar, Vinod Vaikuntanathan, and Anantha Chandrakasan. “GAZELLE: A low latency framework for secure neural network inference”. In: *27th USENIX Security Symposium (USENIX Security 18)*. 2018, pp. 1651–1669.
- [36] William Kahan. “IEEE standard 754 for binary floating-point arithmetic”. In: *Lecture Notes on the Status of IEEE 754.94720-1776* (1996), p. 11.
- [37] Georgios Kaissis et al. “End-to-end privacy preserving deep learning on multi-institutional medical imaging”. In: *Nature Machine Intelligence* 3.6 (2021), pp. 473–484.
- [38] Jonathan Katz. “Universally composable multi-party computation using tamper-proof hardware”. In: *Annual International Conference on the Theory and Applications of Cryptographic Techniques*. Springer. 2007, pp. 115–128.
- [39] Kyungtae Kim et al. “Vessels: Efficient and scalable deep learning prediction on trusted processors”. In: *Proceedings of the 11th ACM Symposium on Cloud Computing*. 2020, pp. 462–476.
- [40] B. Knott et al. “CrypTen: Secure Multi-Party Computation Meets Machine Learning”. In: *arXiv 2109.00984*. 2021.
- [41] Alex Krizhevsky, Vinod Nair, and Geoffrey Hinton. “The CIFAR-10 dataset”. In: *online: http://www.cs.toronto.edu/kriz/cifar.html* 55.5 (2014).
- [42] Alex Krizhevsky, Ilya Sutskever, and Geoffrey E Hinton. “Imagenet classification with deep convolutional neural networks”. In: *Advances in neural information processing systems* 25 (2012).
- [43] Nishant Kumar et al. “Cryptflow: Secure tensorflow inference”. In: *2020 IEEE Symposium on Security and Privacy (SP)*. IEEE. 2020, pp. 336–353.
- [44] Dayeol Lee et al. “Keystone: An open framework for architecting trusted execution environments”. In: *Proceedings of the Fifteenth European Conference on Computer Systems*. 2020, pp. 1–16.
- [45] Jaehyuk Lee et al. “Hacking in darkness: Return-oriented programming against secure enclaves”. In: *26th USENIX Security Symposium (USENIX Security 17)*. 2017, pp. 523–539.
- [46] Sangho Lee et al. “Inferring fine-grained control flow inside SGX enclaves with branch shadowing”. In: *26th USENIX Security Symposium (USENIX Security 17)*. 2017, pp. 557–574.
- [47] Jian Liu et al. “Oblivious neural network predictions via minion transformations”. In: *Proceedings of the 2017 ACM SIGSAC conference on computer and communications security*. 2017, pp. 619–631.
- [48] Yibiao Lu et al. “Correlated Randomness Teleportation via Semi-trusted Hardware—Enabling Silent Multi-party Computation”. In: *European Symposium on Research in Computer Security*. Springer. 2021, pp. 699–720.
- [49] Sébastien Marcel and Yann Rodriguez. “Torchvision the machine-vision package of torch”. In: *Proceedings of the 18th ACM international conference on Multimedia*. 2010, pp. 1485–1488.
- [50] Stephen Merity et al. “Pointer sentinel mixture models”. In: *arXiv preprint arXiv:1609.07843* (2016).
- [51] Pratyush Mishra et al. “Delphi: A cryptographic inference service for neural networks”. In: *29th USENIX Security Symposium (USENIX Security 20)*. 2020, pp. 2505–2522.
- [52] Samer Moein et al. “Hardware attack mitigation techniques analysis”. In: *International Journal on Cryptography and Information Security (IJCIS)* 7.1 (2017), pp. 9–28.
- [53] Daniel Moghimi et al. “TPM-FAIL: TPM meets timing and lattice attacks”. In: *Proceedings of the 29th USENIX Security Symposium*. 2020.
- [54] Payman Mohassel and Peter Rindal. “ABY3: A mixed protocol framework for machine learning”. In: *Proceedings of the 2018 ACM SIGSAC conference on computer and communications security*. 2018, pp. 35–52.
- [55] Payman Mohassel and Yupeng Zhang. “Secureml: A system for scalable privacy-preserving machine learning”. In: *2017 IEEE symposium on security and privacy (SP)*. IEEE. 2017, pp. 19–38.
- [56] Lucien KL Ng and Sherman SM Chow. “{GForce}:{GPU-Friendly} Oblivious and Rapid Neural Network Inference”. In: *30th USENIX Security Symposium (USENIX Security 21)*. 2021, pp. 2147–2164.
- [57] Lucien KL Ng et al. “Goten: Gpu-outsourcing trusted execution of neural network training”. In: *Proceedings of the AAAI Conference on Artificial Intelligence*. Vol. 35. 17. 2021, pp. 14876–14883.
- [58] Olga Ohrimenko et al. “Oblivious Multi-Party Machine Learning on Trusted Processors”. In: *25th USENIX Security Symposium (USENIX Security 16)*. 2016, pp. 619–636.
- [59] Arpita Patra and Ajith Suresh. “BLAZE: blazing fast privacy-preserving machine learning”. In: *arXiv preprint arXiv:2005.09042* (2020).
- [60] Siani Pearson and Boris Balacheff. *Trusted computing platforms: TCPA technology in context*. Prentice Hall Professional, 2003.
- [61] Shahed E Quadir et al. “A survey on chip to system reverse engineering”. In: *ACM journal on emerging technologies in computing systems (JETC)* 13.1 (2016), pp. 1–34.
- [62] Prashanthi Ramachandran et al. “S++: A fast and deployable secure-computation framework for privacy-preserving neural network training”. In: *arXiv preprint arXiv:2101.12078* (2021).
- [63] Wolfgang Rankl and Wolfgang Effing. *Smart card handbook*. John Wiley & Sons, 2004.
- [64] M Sadegh Riazi et al. “Chameleon: A hybrid secure computation framework for machine learning applications”. In: *Proceedings of the 2018 on Asia conference on computer and communications security*. 2018, pp. 707–721.
- [65] M Sadegh Riazi et al. “XONN: XNOR-based Oblivious Deep Neural Network Inference”. In: *28th USENIX Security Symposium (USENIX Security 19)*. 2019, pp. 1501–1518.
- [66] Olga Russakovsky et al. “ImageNet Large Scale Visual Recognition Challenge”. In: *International Journal of Computer Vision (IJCV)* 115.3 (2015), pp. 211–252. DOI: [10.1007/s11263-015-0816-y](https://doi.org/10.1007/s11263-015-0816-y).
- [67] Théo Ryffel et al. “Ariann: Low-interaction privacy-preserving deep learning via function secret sharing”. In: *Proceedings on Privacy Enhancing Technologies 2022.1* (2020), pp. 291–316.

- [68] AMD SEV-SNP. “Strengthening VM isolation with integrity protection and more”. In: *White Paper, January* (2020).
- [69] Shweta Shinde et al. “Preventing your faults from telling your secrets: Defenses against pigeonhole attacks”. In: *arXiv preprint arXiv:1506.04832* (2015).
- [70] Karen Simonyan and Andrew Zisserman. “Very deep convolutional networks for large-scale image recognition”. In: *arXiv preprint arXiv:1409.1556* (2014).
- [71] Sergei Skorobogatov. “How microprobing can attack encrypted memory”. In: *2017 Euromicro Conference on Digital System Design (DSD)*. IEEE, 2017, pp. 244–251.
- [72] Sergei P Skorobogatov and Ross J Anderson. “Optical fault induction attacks”. In: *Cryptographic Hardware and Embedded Systems-CHES 2002: 4th International Workshop Redwood Shores, CA, USA, August 13–15, 2002 Revised Papers 4*. Springer, 2003, pp. 2–12.
- [73] Evan R Sparks and Evan R Sparks. “A security assessment of trusted platform modules computer science technical report TR2007-597”. In: *Dept. Comput. Sci., Dartmouth College, Hanover, NH, USA, Tech. Rep., TR2007-597* (2007).
- [74] Alin Suciu and Tudor Carean. “Benchmarking the true random number generator of TPM chips”. In: *arXiv preprint arXiv:1008.2223* (2010).
- [75] Inc. Synopsys. *Synopsys tRoot Hardware Secure Modules*. URL: <https://www.synopsys.com/designware-ip/security-ip/root-of-trust.html> (visited on 10/03/2022).
- [76] Florian Tramer and Dan Boneh. “Slalom: Fast, verifiable and private execution of neural networks in trusted hardware”. In: *arXiv preprint arXiv:1806.03287* (2018).
- [77] *Trusted Platform Module with SPI based on 32-bit ARM@ SecurCore@ SC300™ CPU*. <https://datasheet.octopart.com/ST33TPM12SPI-STMicroelectronics-datasheet-62334860.pdf>. Nov. 2013.
- [78] Jo Van Bulck, Frank Piessens, and Raoul Strackx. “SGX-Step: A practical attack framework for precise enclave execution control”. In: *Proceedings of the 2nd Workshop on System Software for Trusted Execution*. 2017, pp. 1–6.
- [79] Jo Van Bulck et al. “Foreshadow: Extracting the Keys to the Intel SGX Kingdom with Transient Out-of-Order Execution”. In: *27th USENIX Security Symposium (USENIX Security 18)*. 2018, pp. 991–1008.
- [80] Ashish Vaswani et al. “Attention is all you need”. In: *Advances in neural information processing systems* 30 (2017).
- [81] Stavros Volos, Kapil Vaswani, and Rodrigo Bruno. “Graviton: Trusted Execution Environments on {GPUs}”. In: *13th USENIX Symposium on Operating Systems Design and Implementation (OSDI 18)*. 2018, pp. 681–696.
- [82] Sameer Wagh, Divya Gupta, and Nishanth Chandran. “SecureNN: 3-Party Secure Computation for Neural Network Training.” In: *Proc. Priv. Enhancing Technol.* 2019.3 (2019), pp. 26–49.
- [83] Sameer Wagh et al. “Falcon: Honest-majority maliciously secure framework for private deep learning”. In: *arXiv preprint arXiv:2004.02229* (2020).
- [84] Jinwen Wang et al. “Interface-based side channel attack against intel SGX”. In: *arXiv preprint arXiv:1811.05378* (2018).
- [85] Yongqin Wang et al. “Characterizing and Improving MPC-based Private Inference for Transformer-based Models”. In: *NeurIPS 2021 Workshop Privacy in Machine Learning*. 2021.
- [86] Thomas Wolf et al. “Transformers: State-of-the-Art Natural Language Processing”. In: *Proceedings of the 2020 Conference on Empirical Methods in Natural Language Processing: System Demonstrations*. Online: Association for Computational Linguistics, Oct. 2020, pp. 38–45. URL: <https://www.aclweb.org/anthology/2020.emnlp-demos.6>.
- [87] Pengfei Wu et al. “Hybrid Trust Multi-party Computation with Trusted Execution Environment”. In: ().
- [88] Yuanzhong Xu, Weidong Cui, and Marcus Peinado. “Controlled-channel attacks: Deterministic side channels for untrusted operating systems”. In: *2015 IEEE Symposium on Security and Privacy*. IEEE, 2015, pp. 640–656.
- [89] Andrew C Yao. “Protocols for secure computations”. In: *23rd annual symposium on foundations of computer science (sfcs 1982)*. IEEE, 1982, pp. 160–164.
- [90] Andrew Chi-Chih Yao. “How to generate and exchange secrets”. In: *27th Annual Symposium on Foundations of Computer Science (sfcs 1986)*. IEEE, 1986, pp. 162–167.
- [91] *ZeroMQ*. <https://github.com/zeromq/libzmq>.
- [92] Wenting Zheng et al. “Helen: Maliciously secure cooperative learning for linear models”. In: *2019 IEEE Symposium on Security and Privacy (SP)*. IEEE, 2019, pp. 724–738.
- [93] Xing Zhou et al. “PPMLAC: high performance chipset architecture for secure multi-party computation”. In: *Proceedings of the 49th Annual International Symposium on Computer Architecture*. 2022, pp. 87–101.

Appendix A. Basic MPC Protocols

Correlated Randomness. A large number of random shares have to be obtained by the parties during the offline phase to reduce the communication cost during the offline phase. The 3-out-of-3 randomness is defined as each P_i holding a share of 0: $\alpha = \llbracket \alpha \rrbracket_1^L + \llbracket \alpha \rrbracket_2^L + \llbracket \alpha \rrbracket_3^L$ where $\alpha = 0$ and P_i holds $\llbracket \alpha \rrbracket_i^L$. They can be efficiently generated locally by a pseudo-random function (PRF). The security of the PRF function indicates that the output of a PRF is computationally indistinguishable (indistinguishable by a computationally bounded adversary) from the output of a truly random function. Given k_i as the key that P_i and P_{i+1} share through a key exchange protocol for each i and F as the PRF that is public to all parties, each P_i can generate shares $\llbracket \alpha \rrbracket_i^L$ as $\llbracket \alpha \rrbracket_i^L = \hat{F}_{k_i}(\text{ctr}) - \hat{F}_{k_i}(\text{ctr})$ with increments of ctr each time this process is invoked.

Input Phase. To construct $\llbracket x \rrbracket^L$ from the generated 3-out-of-3 randomness and \bar{x} which is provided by P_i , P_i compute $\llbracket x \rrbracket_i^L = x + \llbracket \alpha \rrbracket_i^L$ and share it with P_{i-1} . P_{i-1} will send $\llbracket \alpha \rrbracket_{i-1}^L$ to P_{i+1} and P_{i+1} will send $\llbracket \alpha \rrbracket_{i+1}^L$ to P_i . In an honest majority malicious setting, additionally P_{i+1} should compute $\llbracket \alpha \rrbracket_{i+1}^L + \llbracket \alpha \rrbracket_{i-1}^L$ and send to P_i , then P_i confirm $\llbracket \alpha \rrbracket_{i+1}^L + \llbracket \alpha \rrbracket_{i-1}^L = -\llbracket \alpha \rrbracket_i^L$, therefore P_{i+1} behaves honestly; P_i should compute $\llbracket \alpha \rrbracket_{i+1}^L + \llbracket \alpha \rrbracket_i^L$ and send to P_{i-1} , then P_{i-1} confirm by $\llbracket \alpha \rrbracket_{i+1}^L + \llbracket \alpha \rrbracket_i^L = -\llbracket \alpha \rrbracket_{i-1}^L$, therefore P_{i+1} behaves honestly. Since P_i is allowed to send an arbitrary input \bar{x} , we do not need to check the share it sends.

Linear Operations. For RSS shared secrets, most linear operations can be performed locally. For shares $\llbracket x \rrbracket^L$, $\llbracket y \rrbracket^L$, and the public scalar c , we have the following:

- $\llbracket x \rrbracket^L + c = (\llbracket x \rrbracket_1^L + c, \llbracket x \rrbracket_2^L, \llbracket x \rrbracket_3^L)$
- $c \cdot \llbracket x \rrbracket^L = (c \cdot \llbracket x \rrbracket_1^L, c \cdot \llbracket x \rrbracket_2^L, c \cdot \llbracket x \rrbracket_3^L)$

• $\llbracket x \rrbracket^L + \llbracket y \rrbracket^L = (\llbracket x \rrbracket_1^L + \llbracket y \rrbracket_1^L, \llbracket x \rrbracket_2^L + \llbracket y \rrbracket_2^L, \llbracket x \rrbracket_3^L + \llbracket y \rrbracket_3^L)$
That can be done without any communication. However, multiplication between shared secrets cannot be done locally.

Reconstruction. $x \leftarrow \Pi_{\text{Reconst}}(\llbracket x \rrbracket^L)$: To reconstruct the plaintext x from the shares $\llbracket x \rrbracket^L$, each party P_i will send $\llbracket x \rrbracket_i^L$ to P_{i+1} in the semi-honest setting. After completion, all parties have all 3 shares to reconstruct x . In a malicious setting, P_i will also send $\llbracket x \rrbracket_{i+1}^L$ to P_{i-1} . Then, under the honest majority assumption, at most one of the two copies of the share they receive is altered. A party can compare the values received from the other two and abort if an inconsistency occurs.

Appendix B. Security Analysis

In this section, we analyze the security of our proposed techniques. The extra or different steps done for a malicious setting than in a semi-honest setting are marked in blue.

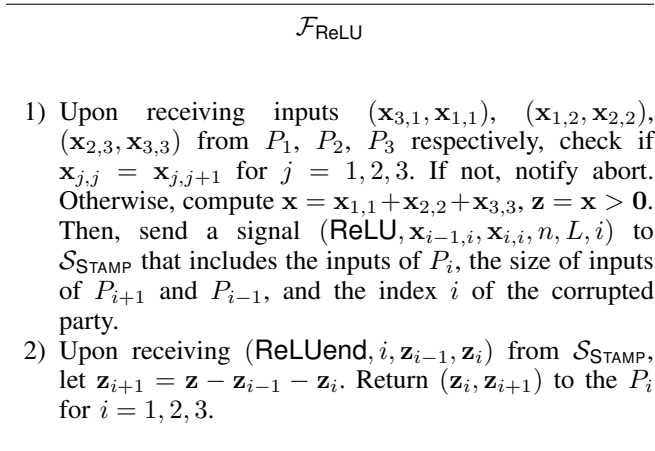


Figure 5: Ideal functionality for Π_{ReLU} .

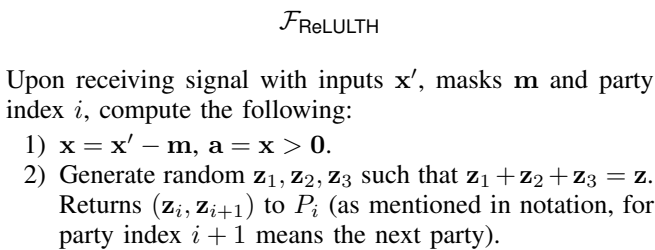


Figure 6: Ideal functionality for the LTH part of Π_{ReLU} .

Proof for Theorem 1. We first prove Theorem 1 of Π_{ReLU} by constructing a simulator $\mathcal{S}_{\text{STAMP}}$ such that no non-uniform PPT environment \mathcal{E} can distinguish between: (i)

the execution of the real protocol $\text{EXEC}_{\Pi_{\text{ReLU}}, \mathcal{A}, \mathcal{E}}$ where parties P_1, P_2, P_3 run Π_{ReLU} and the corrupted parties are controlled by a dummy adversary \mathcal{A} who simply forward messages from/to \mathcal{E} , and (ii) the ideal execution $\text{EXEC}_{\mathcal{F}_{\text{ReLU}}, \mathcal{S}_{\text{STAMP}}, \mathcal{E}}$ where parties interact with $\mathcal{F}_{\text{ReLU}}$, while the simulator $\mathcal{S}_{\text{STAMP}}$ has the control over the corrupted party. Compared to the semi-honest scheme, the changed actions are written in blue.

The Environment \mathcal{E} . The environment \mathcal{E} provides inputs $(\mathbf{x}_{3,1}, \mathbf{x}_{1,1})$ to P_1 , $(\mathbf{x}_{1,2}, \mathbf{x}_{2,2})$ to P_2 , $(\mathbf{x}_{2,3}, \mathbf{x}_{3,3})$ to P_3 , which are forwarded to the ideal functionality $\mathcal{F}_{\text{ReLU}}$ in Figure 5. The environment \mathcal{E} also indicates which party is corrupted to the ideal functionality.

Case 1: P_1 is corrupted ($i = 1$) and P_2, P_3 are honest.

The Simulator. $\mathcal{S}_{\text{STAMP}}$ simulates the following interactions on receiving the signal from $\mathcal{F}_{\text{ReLU}}$:

- Upon receiving $(\text{ReLU}, 1, \mathbf{x}_{3,1}, \mathbf{x}_{1,1}, n, L)$ from $\mathcal{F}_{\text{ReLU}}$, $\mathcal{S}_{\text{STAMP}}$ generates a random $\hat{\mathbf{x}}_2$, and use $(\mathbf{x}_{1,1}, \hat{\mathbf{x}}_2)$ and $(\hat{\mathbf{x}}_2, \mathbf{x}_{3,1})$ as dummy inputs for P_2 and P_3 , respectively.
- $\mathcal{S}_{\text{STAMP}}$ acts as $\mathcal{F}_{\text{GenMask}}$ to generate random masks \mathbf{m}_3 for P_1 and P_3 , then computes $\mathbf{x}'_3 = \mathbf{x}_{3,1} + \mathbf{m}_3$ and sends $(\mathbf{m}_3, \mathbf{x}'_3)$ to P_1 , computes $\mathbf{x}''_3 = \mathbf{x}_{3,1} + \mathbf{m}_3$ and sends $(\mathbf{m}_3, \mathbf{x}''_3)$ to P_3 then also sends $\hat{\mathbf{x}}'_3$ (as adversary input for P_1) and \mathbf{x}''_3 to P_2 on behalf of P_1 and P_3 , respectively.

$\mathcal{S}_{\text{STAMP}}$ also acts as $\mathcal{F}_{\text{GenMask}}$ to generate random masks \mathbf{m}_2 for P_3 and P_2 , then computes $\hat{\mathbf{x}}'_2 = \hat{\mathbf{x}}_2 + \mathbf{m}_2$ and sends $(\mathbf{m}_2, \hat{\mathbf{x}}'_2)$ to P_3 , computes $\mathbf{x}''_2 = \hat{\mathbf{x}}_2 + \mathbf{m}_2$ and sends $(\mathbf{m}_2, \mathbf{x}''_2)$ to P_2 then also sends $\hat{\mathbf{x}}'_2$ and \mathbf{x}''_2 to P_1 on behalf of P_3 and P_2 , respectively.

- $\mathcal{S}_{\text{STAMP}}$ check $\mathbf{x}'_3 = \hat{\mathbf{x}}'_3$, $\mathbf{x}''_3 = \mathbf{x}''_3$ on behalf of P_2 and P_1 respectively, signal abort to $\mathcal{F}_{\text{ReLU}}$ if inconsistency found.
- $\mathcal{S}_{\text{STAMP}}$ acts as $\mathcal{F}_{\text{LTHReLU}}$ with P_2 's input $\hat{\mathbf{x}} = \mathbf{x}'_3 + \hat{\mathbf{x}}_2 + \mathbf{x}_{1,1}$ to (re)generate \mathbf{m}_3 , randoms $\mathbf{z}_1^*, \mathbf{z}_2^*, \mathbf{z}_3$ such that $\mathbf{z}_1^* + \mathbf{z}_2^* + \mathbf{z}_3 = \mathbf{0}$, and then compute $(\mathbf{z}_1, \mathbf{z}_2) = (\text{ReLU}(\hat{\mathbf{x}} - \mathbf{m}_3) + \mathbf{z}_1^*, \mathbf{z}_2^*)$. $\mathcal{S}_{\text{STAMP}}$ sends $(\mathbf{z}_1, \mathbf{z}_2)$ to P_2 . $\mathcal{S}_{\text{STAMP}}$ sends $\tilde{\mathbf{z}}_1$ to P_1 and sends \mathbf{z}_2 to P_3 (on behalf P_2).

$\mathcal{S}_{\text{STAMP}}$ acts as $\mathcal{F}_{\text{LTHReLU}}$ with P_1 's input $\hat{\mathbf{x}}' = \mathbf{x}'_2 + \mathbf{x}_{3,1} + \mathbf{x}_{1,1}$ to (re)generate \mathbf{m}_2 , randoms $\mathbf{z}_1^*, \mathbf{z}_2^*, \mathbf{z}_3$ such that $\mathbf{z}_1^* + \mathbf{z}_2^* + \mathbf{z}_3 = \mathbf{0}$, and then compute $(\mathbf{z}_3, \mathbf{z}'_1) = (\mathbf{z}_3, \text{ReLU}(\hat{\mathbf{x}}' - \mathbf{m}_3) + \mathbf{z}_1^*)$. $\mathcal{S}_{\text{STAMP}}$ sends $(\mathbf{z}_3, \mathbf{z}'_1)$ to P_1 . $\mathcal{S}_{\text{STAMP}}$ sends $\tilde{\mathbf{z}}_3$ to P_3 and sends $\tilde{\mathbf{z}}'_1$ to P_2 (as adversary inputs on behalf P_1).

- $\mathcal{S}_{\text{STAMP}}$ acts as $\mathcal{F}_{\text{GenMaskShr}}$ for P_1 to (re)generate random \mathbf{z}_3 and sends it to P_1 . Similarly, $\mathcal{S}_{\text{STAMP}}$ acts as $\mathcal{F}_{\text{GenMaskShr}}$ for P_3 to (re)generate random as \mathbf{z}_3 and sends it to P_3 . $\mathcal{S}_{\text{STAMP}}$ also generate \mathbf{z}_2^* for P_2 and P_3 .
- $\mathcal{S}_{\text{STAMP}}$ checks if $\mathbf{z}'_1 = \mathbf{z}_1$ received by P_1 , also P_2 ; if same \mathbf{z}_2^* received by P_2 , also P_3 ; if same \mathbf{z}_3 received by P_3 , also P_1 . Signal abort to $\mathcal{F}_{\text{ReLU}}$ if an inconsistency is found. If no abort is signaled, $\mathcal{S}_{\text{STAMP}}$ signals $(\text{ReLUend}, 1, \mathbf{z}_3, \mathbf{z}_1)$ to $\mathcal{F}_{\text{ReLU}}$.

Indistinguishability. We prove the indistinguishability argument by constructing a sequence of hybrid games as follows.

Hybrid \mathcal{H}_0 : This is the real protocol execution.

Hybrid \mathcal{H}_1 : \mathcal{H}_1 is the same as \mathcal{H}_0 , except that we replace $\Pi_{\text{LTH.GenMask}}$ with simulated $\mathcal{F}_{\text{GenMask}}$ that outputs random $\hat{\mathbf{m}}_3, \hat{\mathbf{m}}_2$ for both step 1) and 4).

We claim that \mathcal{H}_0 and \mathcal{H}_1 are computationally indistinguishable. This is because $\Pi_{\text{LTH.GenMask}}$ generates pseudo-random $\mathbf{m}_3, \mathbf{m}_2$ to P_1 using LTH. Due to the secure hardware assumption, there exists a simulator that is indistinguishable from the real hardware protocol execution. Moreover, due to the security of PRF used in LTH, the random $\mathbf{m}_3, \mathbf{m}_2$ produced by LTH is computationally indistinguishable from the random $\hat{\mathbf{m}}_3, \hat{\mathbf{m}}_2$ generated by the simulator. Therefore, \mathcal{H}_0 and \mathcal{H}_1 are computationally indistinguishable.

Hybrid \mathcal{H}_2 : \mathcal{H}_2 is the same as \mathcal{H}_1 , except that we replace step 4) with the simulated $\mathcal{F}_{\text{LTHReLU}}$.

We claim that \mathcal{H}_1 and \mathcal{H}_2 are computationally indistinguishable using the same argument on the trusted hardware and PRF security as in \mathcal{H}_1 . Specifically, the random vectors generated by $\Pi_{\text{LTH.GenMaskShare}}$ in the LTH are based on PRF and therefore, they are computationally indistinguishable from the random vectors generated by the simulator. Therefore, \mathcal{H}_1 and \mathcal{H}_2 are computationally indistinguishable.

Hybrid \mathcal{H}_3 : \mathcal{H}_3 is the same as \mathcal{H}_2 , except that P_2, P_3 use dummy inputs for interaction, instead of the ones provided by the environment. In this hybrid, we introduce an ideal functionality $\mathcal{F}_{\text{ReLU}}$ that takes the environments' actual inputs and returns the corresponding outputs.

We claim that \mathcal{H}_2 and \mathcal{H}_3 are indistinguishable. Since the corrupted party is P_1 , $\mathcal{S}_{\text{STAMP}}$ knows $\mathbf{x}_{3,1} = \mathbf{x}_{3,3}, \mathbf{x}_{1,1} = \mathbf{x}_{1,2}$. The dummy inputs would be $\mathbf{x}_{2,2} = \mathbf{x}_{2,3}$ (represented by $\hat{\mathbf{x}}_2$ in $\mathcal{S}_{\text{STAMP}}$). The distribution of the computation result, $\hat{\mathbf{x}} = \mathbf{x}'_3 + \hat{\mathbf{x}}_2 + \mathbf{x}_{1,1} = (\mathbf{x}_{3,1} + \mathbf{m}_3) + \hat{\mathbf{x}}_2 + \mathbf{x}_{1,1}$ and $\hat{\mathbf{x}}' = \mathbf{x}'_2 + \mathbf{x}_{3,1} + \mathbf{x}_{1,1} = (\hat{\mathbf{x}}_2 + \mathbf{m}_2) + \mathbf{x}_{3,1} + \mathbf{x}_{1,1}$ are uniformly random since $\mathbf{m}_3, \mathbf{m}_2$ are random. Therefore, \mathcal{H}_2 and \mathcal{H}_3 are indistinguishable.

The adversary's view of \mathcal{H}_3 is identical to $\text{EXEC}_{F, \mathcal{S}_{\text{STAMP}}, \mathcal{E}}$. Therefore, in **Case 1** the view of \mathcal{A} and \mathcal{E} are indistinguishable in the real and the simulated world.

Putting it all together, we have that $\mathcal{H}_0 \approx \mathcal{H}_1 \approx \mathcal{H}_2 \approx \mathcal{H}_3 = \mathcal{S}_{\text{STAMP}}$.

Case 2: P_2 is corrupted ($i = 2$) and P_1, P_3 are honest.

The Simulator. $\mathcal{S}_{\text{STAMP}}$ simulates the following interactions on receiving the signal from $\mathcal{F}_{\text{ReLU}}$:

- Upon receiving $(\text{ReLU}, 2, \mathbf{x}_{1,2}, \mathbf{x}_{2,2}, n, L)$ from $\mathcal{F}_{\text{ReLU}}$, $\mathcal{S}_{\text{STAMP}}$ generates a random $\hat{\mathbf{x}}_3$, and use $(\mathbf{x}_{2,2}, \hat{\mathbf{x}}_3)$ and $(\hat{\mathbf{x}}_3, \mathbf{x}_{1,2})$ as dummy inputs for P_3 and P_1 , respectively.
- $\mathcal{S}_{\text{STAMP}}$ acts as $\mathcal{F}_{\text{GenMask}}$ to generate random masks \mathbf{m}_3 for P_1 and P_3 , then computes $\mathbf{x}'_3 = \hat{\mathbf{x}}_3 + \mathbf{m}_3$ and sends $(\mathbf{m}_3, \mathbf{x}'_3)$ to P_1 , computes $\mathbf{x}''_3 = \hat{\mathbf{x}}_3 + \mathbf{m}_3$ and sends $(\mathbf{m}_3, \mathbf{x}''_3)$ to P_3 then also sends \mathbf{x}'_3 and \mathbf{x}''_3 to P_2 on behalf of P_1 and P_3 , respectively.

$\mathcal{S}_{\text{STAMP}}$ also acts as $\mathcal{F}_{\text{GenMask}}$ to generate random masks \mathbf{m}_2 for P_3 and P_2 , then computes $\mathbf{x}'_2 = \mathbf{x}_{2,2} + \mathbf{m}_2$ and sends $(\mathbf{m}_2, \mathbf{x}'_2)$ to P_3 , computes $\mathbf{x}''_2 = \mathbf{x}_{2,2} + \mathbf{m}_2$ and sends $(\mathbf{m}_2, \mathbf{x}''_2)$ to P_2 then also sends \mathbf{x}'_2 and \mathbf{x}''_2 (as

adversary input for P_3) to P_1 on behalf of P_3 and P_2 , respectively.

- $\mathcal{S}_{\text{STAMP}}$ check $\mathbf{x}'_3 = \mathbf{x}''_3, \hat{\mathbf{x}}'_2 = \mathbf{x}'_2$ on behalf of P_2 and P_1 respectively, signal abort to $\mathcal{F}_{\text{ReLU}}$ if inconsistency found.
- $\mathcal{S}_{\text{STAMP}}$ acts as $\mathcal{F}_{\text{LTHReLU}}$ with P_2 's input $\hat{\mathbf{x}} = \mathbf{x}'_3 + \mathbf{x}_{2,2} + \mathbf{x}_{1,2}$ to (re)generate \mathbf{m}_3 , randoms $\mathbf{z}_1^*, \mathbf{z}_2, \mathbf{z}_3^*$ such that $\mathbf{z}_1^* + \mathbf{z}_2 + \mathbf{z}_3^* = 0$, and then compute $(\mathbf{z}_1, \mathbf{z}_2) = (\text{ReLU}(\hat{\mathbf{x}} - \mathbf{m}_3) + \mathbf{z}_1^*, \mathbf{z}_2)$. $\mathcal{S}_{\text{STAMP}}$ sends $(\mathbf{z}_1, \mathbf{z}_2)$ to P_2 . $\mathcal{S}_{\text{STAMP}}$ sends $\bar{\mathbf{z}}_1$ to P_1 and sends $\bar{\mathbf{z}}_2$ to P_3 (as adversary inputs for P_2).
- $\mathcal{S}_{\text{STAMP}}$ acts as $\mathcal{F}_{\text{LTHReLU}}$ with P_1 's input $\hat{\mathbf{x}}' = \mathbf{x}'_2 + \hat{\mathbf{x}}_3 + \mathbf{x}_{1,2}$, (re)generate \mathbf{m}_2 , generate randoms $\mathbf{z}_1^*, \mathbf{z}_2, \mathbf{z}_3^*$ such that $\mathbf{z}_1^* + \mathbf{z}_2 + \mathbf{z}_3^* = 0$, and then compute $(\mathbf{z}_3, \mathbf{z}'_1) = (\mathbf{z}_3^*, \text{ReLU}(\hat{\mathbf{x}}' - \mathbf{m}_2) + \mathbf{z}_1^*)$. $\mathcal{S}_{\text{STAMP}}$ sends $(\mathbf{z}_3, \mathbf{z}'_1)$ to P_1 . $\mathcal{S}_{\text{STAMP}}$ sends \mathbf{z}_3 to P_3 and sends \mathbf{z}'_1 to P_2 (on behalf of P_1).
- $\mathcal{S}_{\text{STAMP}}$ acts as $\mathcal{F}_{\text{GenMaskShr}}$ for P_1 to (re)generate random \mathbf{z}_3^* and sends it to P_1 . Similarly, $\mathcal{S}_{\text{STAMP}}$ acts as $\mathcal{F}_{\text{GenMaskShr}}$ for P_3 to (re)generate random \mathbf{z}_3^* and sends it to P_3 . $\mathcal{S}_{\text{STAMP}}$ also generate \mathbf{z}_2 for P_2 and P_3 .
- $\mathcal{S}_{\text{STAMP}}$ checks if $\mathbf{z}'_1 = \bar{\mathbf{z}}_1$ received by P_1 , also P_2 ; if same \mathbf{z}_2 received by P_2 , also P_3 ; if same \mathbf{z}_3^* received by P_3 , also P_1 . Signal abort to $\mathcal{F}_{\text{ReLU}}$ if an inconsistency is found. If no abort is signaled, $\mathcal{S}_{\text{STAMP}}$ signals $(\text{ReLUend}, 2, \mathbf{z}_1, \mathbf{z}_2)$ to $\mathcal{F}_{\text{ReLU}}$.

Indistinguishability. We prove the indistinguishability argument by constructing a sequence of hybrid games as follows. Notice that the first 3 games, **Hybrid \mathcal{H}_0** , **Hybrid \mathcal{H}_1** and **Hybrid \mathcal{H}_2** are identical as **Case 1**'s. The proofs between **Hybrid \mathcal{H}_0** and **Hybrid \mathcal{H}_1** , **Hybrid \mathcal{H}_1** and **Hybrid \mathcal{H}_2** are exactly the same.

Hybrid \mathcal{H}_3 : \mathcal{H}_3 is the same as \mathcal{H}_2 , except that P_1, P_3 use dummy inputs for interaction, instead of the ones provided by the environment. In this hybrid, we introduce an ideal functionality $\mathcal{F}_{\text{ReLU}}$ that takes the environments' actual inputs and returns the corresponding outputs.

We claim that \mathcal{H}_2 and \mathcal{H}_3 are indistinguishable. Since the corrupted party is P_2 , $\mathcal{S}_{\text{STAMP}}$ knows $\mathbf{x}_{2,2} = \mathbf{x}_{2,3}, \mathbf{x}_{1,2} = \mathbf{x}_{1,1}$. The dummy inputs would be $\mathbf{x}_{3,3} = \mathbf{x}_{1,3}$ (represented by $\hat{\mathbf{x}}_3$ in $\mathcal{S}_{\text{STAMP}}$). The distribution of the computation result, $\hat{\mathbf{x}} = \mathbf{x}'_3 + \mathbf{x}_{2,2} + \mathbf{x}_{1,2} = (\hat{\mathbf{x}}_3 + \mathbf{m}_3) + \mathbf{x}_{2,2} + \mathbf{x}_{1,2}$ and $\hat{\mathbf{x}}' = \mathbf{x}'_2 + \hat{\mathbf{x}}_3 + \mathbf{x}_{1,2} = (\hat{\mathbf{x}}_{2,2} + \mathbf{m}_3) + \hat{\mathbf{x}}_3 + \mathbf{x}_{1,2}$ are uniformly random since $\mathbf{m}_3, \mathbf{m}_2$ are random. Therefore, \mathcal{H}_2 and \mathcal{H}_3 are indistinguishable.

The adversary's view of \mathcal{H}_3 is identical to $\text{EXEC}_{F, \mathcal{S}_{\text{STAMP}}, \mathcal{E}}$. Therefore, in **Case 2** the view of \mathcal{A} and \mathcal{E} are indistinguishable in the real and the simulated world.

Putting it all together, we have that $\mathcal{H}_0 \approx \mathcal{H}_1 \approx \mathcal{H}_2 \approx \mathcal{H}_3 = \mathcal{S}_{\text{STAMP}}$.

Case 3: P_3 is corrupted ($i = 3$) and P_1, P_2 are honest.

The Simulator. $\mathcal{S}_{\text{STAMP}}$ simulates the following interactions on receiving the signal from $\mathcal{F}_{\text{ReLU}}$:

- Upon receiving $(\text{ReLU}, 3, \mathbf{x}_{2,3}, \mathbf{x}_{3,3}, n, L)$ from $\mathcal{F}_{\text{ReLU}}$, $\mathcal{S}_{\text{STAMP}}$ generates a random $\hat{\mathbf{x}}_1$, and use $(\mathbf{x}_{3,3}, \hat{\mathbf{x}}_1)$ and $(\hat{\mathbf{x}}_1, \mathbf{x}_{2,3})$ as dummy inputs for P_1 and P_2 , respectively.

- $\mathcal{S}_{\text{STAMP}}$ acts as $\mathcal{F}_{\text{GenMask}}$ to generate random masks \mathbf{m}_3 for P_1 and P_3 , then computes $\mathbf{x}'_3 = \mathbf{x}_{3,3} + \mathbf{m}_3$ and sends $(\mathbf{m}_3, \mathbf{x}'_3)$ to P_1 , computes $\mathbf{x}''_3 = \mathbf{x}_{3,3} + \mathbf{m}_3$ and sends $(\mathbf{m}_3, \mathbf{x}''_3)$ to P_3 then also sends \mathbf{x}'_3 and arbitrary $\tilde{\mathbf{x}}''_3$ to P_2 on behalf of P_1 and P_3 , respectively. $\mathcal{S}_{\text{STAMP}}$ also acts as $\mathcal{F}_{\text{GenMask}}$ to generate random masks \mathbf{m}_2 for P_3 and P_2 , then computes $\mathbf{x}'_2 = \mathbf{x}_{2,3} + \mathbf{m}_2$ and sends $(\mathbf{m}_2, \mathbf{x}'_2)$ to P_3 , computes $\mathbf{x}''_2 = \mathbf{x}_{2,3} + \mathbf{m}_2$ and sends $(\mathbf{m}_2, \mathbf{x}''_2)$ to P_2 then also sends $\tilde{\mathbf{x}}''_2$ (as adversary input for P_3) and \mathbf{x}''_2 to P_1 on behalf of P_3 and P_2 , respectively.
- $\mathcal{S}_{\text{STAMP}}$ check $\tilde{\mathbf{x}}''_3 = \mathbf{x}'_3$, $\mathbf{x}''_2 = \tilde{\mathbf{x}}''_2$ on behalf of P_2 and P_1 respectively, signal abort to $\mathcal{F}_{\text{ReLU}}$ if inconsistency found.
- $\mathcal{S}_{\text{STAMP}}$ acts as $\mathcal{F}_{\text{LTHReLU}}$ with P_2 's input $\hat{\mathbf{x}} = \mathbf{x}'_3 + \mathbf{x}_{2,3} + \hat{\mathbf{x}}_1$ to (re)generate \mathbf{m}_3 , randoms $\mathbf{z}_1^*, \mathbf{z}_2, \mathbf{z}_3$ such that $\mathbf{z}_1^* + \mathbf{z}_2 + \mathbf{z}_3 = 0$, and then compute $(\mathbf{z}_1^{**}, \mathbf{z}_2) = (\text{ReLU}(\hat{\mathbf{x}} - \mathbf{m}_3) + \mathbf{z}_1^*, \mathbf{z}_2)$. $\mathcal{S}_{\text{STAMP}}$ sends $(\mathbf{z}_1^{**}, \mathbf{z}_2)$ to P_2 . $\mathcal{S}_{\text{STAMP}}$ sends \mathbf{z}_1^{**} to P_1 and sends \mathbf{z}_2 to P_3 (on behalf P_2).
- $\mathcal{S}_{\text{STAMP}}$ acts as $\mathcal{F}_{\text{LTHReLU}}$ with P_1 's input $\hat{\mathbf{x}}' = \mathbf{x}'_2 + \hat{\mathbf{x}}_1 + \mathbf{x}_{3,3}$, (re)generate \mathbf{m}_2 , generate randoms $\mathbf{z}_1^*, \mathbf{z}_2, \mathbf{z}_3$ such that $\mathbf{z}_1^* + \mathbf{z}_2 + \mathbf{z}_3 = 0$, and then compute $(\mathbf{z}_3, \mathbf{z}'_1) = (\mathbf{z}_3, \text{ReLU}(\hat{\mathbf{x}}' - \mathbf{m}_2) + \mathbf{z}_1^*)$. $\mathcal{S}_{\text{STAMP}}$ sends $(\mathbf{z}_3, \mathbf{z}'_1)$ to P_1 . $\mathcal{S}_{\text{STAMP}}$ sends \mathbf{z}_3 to P_3 and sends \mathbf{z}'_1 to P_2 (on behalf P_1).
- $\mathcal{S}_{\text{STAMP}}$ acts as $\mathcal{F}_{\text{GenMaskShr}}$ for P_1 to (re)generate random \mathbf{z}_3 and sends it to P_1 . Similarly, $\mathcal{S}_{\text{STAMP}}$ acts as $\mathcal{F}_{\text{GenMaskShr}}$ for P_3 to (re)generate random \mathbf{z}_3 and sends it to P_3 . $\mathcal{S}_{\text{STAMP}}$ also generate \mathbf{z}_2 for P_2 and P_3 .
- $\mathcal{S}_{\text{STAMP}}$ checks if $\mathbf{z}'_1 = \mathbf{z}_1^{**}$ received by P_1 , also P_2 ; if same \mathbf{z}_2 received by P_2 , also P_3 ; if same \mathbf{z}_3 received by P_3 , also P_1 . Signal abort to $\mathcal{F}_{\text{ReLU}}$ if an inconsistency is found. If no abort is signaled, $\mathcal{S}_{\text{STAMP}}$ signals $(\text{ReLUend}, 3, \mathbf{z}_2, \mathbf{z}_3)$ to $\mathcal{F}_{\text{ReLU}}$.

Indistinguishability. We prove the indistinguishability argument by constructing a sequence of hybrid games as follows. Notice that the first 3 games, **Hybrid** \mathcal{H}_0 , **Hybrid** \mathcal{H}_1 and **Hybrid** \mathcal{H}_2 are identical as **Case 1**'s. The proofs between **Hybrid** \mathcal{H}_0 and **Hybrid** \mathcal{H}_1 , **Hybrid** \mathcal{H}_1 and **Hybrid** \mathcal{H}_2 are exactly the same.

Hybrid \mathcal{H}_3 : \mathcal{H}_3 is the same as \mathcal{H}_2 , except that P_1, P_3 use dummy inputs for interaction, instead of the ones provided by the environment. In this hybrid, we introduce an ideal functionality $\mathcal{F}_{\text{ReLU}}$ that takes the environments' actual inputs and returns the corresponding outputs.

We claim that \mathcal{H}_2 and \mathcal{H}_3 are indistinguishable. Since the corrupted party is P_2 , $\mathcal{S}_{\text{STAMP}}$ knows $\mathbf{x}_{2,3} = \mathbf{x}_{2,2}, \mathbf{x}_{3,3} = \mathbf{x}_{3,1}$. The dummy inputs would be $\mathbf{x}_{1,1} = \mathbf{x}_{1,2}$ (represented by $\hat{\mathbf{x}}_1$ in $\mathcal{S}_{\text{STAMP}}$). The distribution of the computation result, $\hat{\mathbf{x}} = \mathbf{x}'_3 + \mathbf{x}_{2,3} + \hat{\mathbf{x}}_1 = (\mathbf{x}_{3,3} + \mathbf{m}_3) + \mathbf{x}_{2,3} + \hat{\mathbf{x}}_1$ and $\hat{\mathbf{x}}' = \mathbf{x}'_2 + \hat{\mathbf{x}}_1 + \mathbf{x}_{3,3} = (\hat{\mathbf{x}}_{2,3} + \mathbf{m}_3) + \hat{\mathbf{x}}_1 + \mathbf{x}_{3,3}$ are uniformly random since $\mathbf{m}_3, \mathbf{m}_2$ are random. Therefore, \mathcal{H}_2 and \mathcal{H}_3 are indistinguishable.

The adversary's view of \mathcal{H}_3 is identical to $\text{EXEC}_{F, \mathcal{S}_{\text{STAMP}}, \mathcal{E}}$. Therefore, in **Case 1** the view of \mathcal{A} and \mathcal{E} are indistinguishable in the real and the simulated world.

Putting it all together, we have that $\mathcal{H}_0 \approx \mathcal{H}_1 \approx \mathcal{H}_2 \approx \mathcal{H}_3 = \mathcal{S}_{\text{STAMP}}$ and this completes the proof. \square

Notice that as discussed in §4.4, the above proof works identically for MaxPooling and BatchNorm since only the plaintext computations after subtracting the masks are different.

Next, we will prove the **Theorem 2**. We provide the complete proof for case 1 (where P_1 is corrupted) due to the space limit, and the proof of the other two cases are similar as provided in the proof for Π_{ReLU} .

$\mathcal{F}_{\text{MatMulReLU}}$

- 1) Upon receiving inputs $(\mathbf{A}_{3,1}, \mathbf{A}_{1,1}, \mathbf{B}_{3,1}, \mathbf{B}_{1,1}), (\mathbf{A}_{1,2}, \mathbf{A}_{2,2}, \mathbf{B}_{1,2}, \mathbf{B}_{2,2}), (\mathbf{A}_{2,3}, \mathbf{A}_{3,3}, \mathbf{B}_{2,3}, \mathbf{B}_{3,3})$ from P_1, P_2, P_3 respectively, check if $\mathbf{A}_{j,j} = \mathbf{A}_{j,j+1}, \mathbf{B}_{j,j} = \mathbf{B}_{j,j+1}$ for $j = 1, 2, 3$. If not, notify abort. Otherwise, compute $\mathbf{C}' = (\mathbf{A}_{1,1} + \mathbf{A}_{2,2} + \mathbf{B}_{3,3}) \times (\mathbf{B}_{1,1} + \mathbf{B}_{2,2} + \mathbf{B}_{3,3}) \gg \text{fp}$, $\mathbf{C} = \mathbf{C}' > \mathbf{0}$. Then, send a signal $(\text{MatMalReLU}, i, \mathbf{A}_{i-1,i}, \mathbf{A}_{i,i}, \mathbf{B}_{i-1,i}, \mathbf{B}_{i,i}, a, b, c, L)$ to $\mathcal{S}_{\text{STAMP}}$ that includes the inputs of P_i , the size of inputs of P_{i+1} and P_{i-1} , and the index i of the corrupted party.
 - 2) Upon receiving $(\text{MatMalReLUend}, i, \mathbf{C}_{i-1}, \mathbf{C}_i)$ from $\mathcal{S}_{\text{STAMP}}$, let $\mathbf{C}_{i+1} = \mathbf{z} - \mathbf{C}_{i-1} - \mathbf{C}_i$. Return $(\mathbf{C}_i, \mathbf{C}_{i+1})$ to the P_i for $i = 1, 2, 3$.
-

Figure 7: Ideal functionality for $\Pi_{\text{MatMulReLU}}$.

$\mathcal{F}_{\text{MatMulReLU LTH}}$

Upon receiving signal with inputs $\hat{\mathbf{C}}'$, masks \mathbf{M} and party index i , compute the following:

- 1) $\mathbf{D} = \hat{\mathbf{C}}' - \mathbf{M}$, $\mathbf{E} = \mathbf{D} > \mathbf{0}$.
 - 2) Generate random $\mathbf{C}_1, \mathbf{C}_2, \mathbf{C}_3$ such that $\mathbf{C}_1 + \mathbf{C}_2 + \mathbf{C}_3 = \mathbf{C}$. Returns $(\mathbf{C}_i, \mathbf{C}_{i+1})$ to P_i (as mentioned in notation, for party index $i + 1$ means the next party).
-

Figure 8: Ideal functionality for the LTH part of Π_{ReLU} .

Proof for Theorem 2. We prove **Theorem 2** by constructing a simulator and a series of hybrid games similar to the Proof of **Theorem 1**, with \mathcal{E} providing inputs to parties.

Case 1: P_1 is corrupted ($i = 1$) and P_2, P_3 are honest.

The Simulator. $\mathcal{S}_{\text{STAMP}}$ simulates the following interactions on receiving the signal from $\mathcal{F}_{\text{MatMalReLU}}$:

- Upon receiving $(\text{MatMalReLU}, 1, \mathbf{A}_{3,1}, \mathbf{A}_{1,1}, \mathbf{B}_{3,1}, \mathbf{B}_{1,1}, a, b, c, L)$ from $\mathcal{F}_{\text{MatMalReLU}}$, $\mathcal{S}_{\text{STAMP}}$ generates random $\hat{\mathbf{A}}_2, \hat{\mathbf{B}}_2$, and use $(\mathbf{A}_{1,1}, \hat{\mathbf{A}}_2, \mathbf{B}_{1,1}, \hat{\mathbf{B}}_2)$ and

$(\hat{\mathbf{A}}_2, \mathbf{A}_{3,1}, \hat{\mathbf{B}}_2, \mathbf{B}_{3,1})$ as dummy inputs for P_2 and P_3 , respectively.

- $\mathcal{S}_{\text{STAMP}}$ invokes the simulator of the secure multiplication protocol $\Pi_{\text{mal-arith-mult}}$ of [54] without the truncation. In the end, $(\hat{\mathbf{C}}_{3,1}, \hat{\mathbf{C}}_1, 1), (\hat{\mathbf{C}}_{1,2}, \hat{\mathbf{C}}_2, 2), (\hat{\mathbf{C}}_{2,3}, \hat{\mathbf{C}}_3, 3)$ are distributed accordingly and $\mathcal{S}_{\text{STAMP}}$ will signal abort to $\mathcal{F}_{\text{MatMulReLU}}$ if inconsistency was found in the distributed shares.
- $\mathcal{S}_{\text{STAMP}}$ acts as $\mathcal{F}_{\text{GenMask}}$ to generate random masks \mathbf{M}_2 for P_2 and P_3 , \mathbf{M}_3 for P_3 and P_1 so that $\mathbf{M}_1 + \mathbf{M}_2 + \mathbf{M}_3 = \mathbf{0}$. Then $\mathcal{S}_{\text{STAMP}}$ computes $\hat{\mathbf{C}}'_{2,2} = \hat{\mathbf{C}}_{2,2} + \mathbf{M}_2$ as P_2 and $\hat{\mathbf{C}}'_{2,3} = \hat{\mathbf{C}}_{2,3} + \mathbf{M}_2$ as P_3 ; $\hat{\mathbf{C}}'_{3,3} = \hat{\mathbf{C}}_{3,3} + \mathbf{M}_3$ as P_3 and $\hat{\mathbf{C}}'_{3,1} = \hat{\mathbf{C}}_{3,1} + \mathbf{M}_3$ as P_1 . $\mathcal{S}_{\text{STAMP}}$ sends $\hat{\mathbf{C}}'_{2,2}, \hat{\mathbf{C}}'_{2,3}$ to P_1 as P_2 and P_3 , sends $\hat{\mathbf{C}}'_{3,3}, \hat{\mathbf{C}}'_{3,1}$ to P_2 as P_3 and P_1 . $\mathcal{S}_{\text{STAMP}}$ aborts if any inconsistency is found on the pairs.
- $\mathcal{S}_{\text{STAMP}}$ computes $\hat{\mathbf{C}}'_1 = \hat{\mathbf{C}}'_{2,2} + \hat{\mathbf{C}}'_{3,1} + \hat{\mathbf{C}}^L_{1,1}$ as P_1 , $\hat{\mathbf{C}}'_2 = \hat{\mathbf{C}}'_{3,3} + \hat{\mathbf{C}}^L_{1,2} + \hat{\mathbf{C}}^L_{2,2}$ as P_2 .
- $\mathcal{S}_{\text{STAMP}}$ acts as $\mathcal{F}_{\text{LTHReLU}}(H_1)$ with P_1 's input $\hat{\mathbf{C}}'_1$ to (re)generate \mathbf{M}_2 , computes $\hat{\mathbf{C}} = (\hat{\mathbf{C}}'_1 - \mathbf{M}_2) \gg \text{fp}$. $\mathcal{S}_{\text{STAMP}}$ computes $\mathbf{D} = \hat{\mathbf{C}} > \mathbf{0}$, generates $\mathbf{Z}'_1 + \mathbf{Z}'_2 + \mathbf{Z}'_3 = \mathbf{0}$ (as $\mathcal{F}_{\text{GenMaskShr}}$), then obtain $(\mathbf{Z}'_3, \mathbf{Z}'_1 + \mathbf{D})$ as $(\mathbf{Z}_{3,1}, \mathbf{Z}_{1,1})$ for P_1 . $\mathcal{S}_{\text{STAMP}}$ acts as $\mathcal{F}_{\text{LTHReLU}}(H_2)$ with P_2 's input $\hat{\mathbf{C}}'_2$ to (re)generate \mathbf{M}_3 , computes $\hat{\mathbf{C}} = (\hat{\mathbf{C}}'_2 - \mathbf{M}_3) \gg \text{fp}$. $\mathcal{S}_{\text{STAMP}}$ computes $\mathbf{D} = \hat{\mathbf{C}} > \mathbf{0}$ (as $\mathcal{F}_{\text{GenMaskShr}}$), generates $\mathbf{Z}'_1 + \mathbf{Z}'_2 + \mathbf{Z}'_3 = \mathbf{0}$, then obtain $(\mathbf{Z}'_1 + \mathbf{D}, \mathbf{Z}'_2)$ as $(\mathbf{Z}_{1,2}, \mathbf{Z}_{2,2})$ for P_1 .
- $\mathcal{S}_{\text{STAMP}}$ acts as $\mathcal{F}_{\text{GenMaskShr}}$ for P_3 to (re)generate $(\mathbf{Z}_{2,3}, \mathbf{Z}_{3,3}) = (\mathbf{Z}'_2, \mathbf{Z}'_3)$ and sends it to P_3 . $\mathcal{S}_{\text{STAMP}}$ compare $\mathbf{Z}_{1,1} = \mathbf{Z}_{1,2}$ as P_1 and P_2 ; $\mathbf{Z}_{2,2} = \mathbf{Z}_{2,3}, \mathbf{Z}_{3,3} = \mathbf{Z}_{3,1}$ as P_3 . Signal abort to $\mathcal{F}_{\text{MatMulReLU}}$ if inconsistency was found.

Indistinguishability. We prove the indistinguishability argument by constructing a sequence of hybrid games as follows.

Hybrid \mathcal{H}_0 : This is the real protocol execution.

Hybrid \mathcal{H}_1 : \mathcal{H}_1 is the same as \mathcal{H}_0 , except that we replace $\Pi_{\text{LTH.GenMask}}$ with simulated $\mathcal{F}_{\text{GenMask}}$ that outputs random $\mathbf{M}_2, \mathbf{M}_3$ for both step 2) and 5).

Hybrid \mathcal{H}_2 : \mathcal{H}_2 is the same as \mathcal{H}_1 , except that we replace step 5) with the simulated $\mathcal{F}_{\text{LTHMatMulReLU}}$.

Proofs of \mathcal{H}_0 and $\mathcal{H}_1, \mathcal{H}_1$ and \mathcal{H}_2 being computationally indistinguishable are similar to the proof of [Theorem 1](#), with the actual random masks replaced by $\mathbf{M}_2, \mathbf{M}_3$.

Hybrid \mathcal{H}_3 : \mathcal{H}_3 is the same as \mathcal{H}_2 , except that P_2, P_3 use dummy inputs for interaction, instead of the ones provided by the environment. Also $\Pi_{\text{mal-arith-mult}}$ of [54] is replaced by its corresponding simulator. In this hybrid, we introduce an ideal functionality $\mathcal{F}_{\text{ReLU}}$ that takes the environments' actual inputs and returns the corresponding outputs.

We claim that \mathcal{H}_2 and \mathcal{H}_3 are indistinguishable. \mathcal{H}_2 and \mathcal{H}_3 are only different in inputs and step 1), and their indistinguishability directly comes from the security of the simulator of $\Pi_{\text{mal-arith-mult}}$. Again we refer the reader to [54] for more details. Since the view of P_1 does not change after step 1), it remains the same for the whole protocol since later

steps remain the same in both hybrids. Therefore, \mathcal{H}_2 and \mathcal{H}_3 are indistinguishable.

The adversary's view of \mathcal{H}_3 is identical to $\text{EXEC}_{\mathcal{F}, \mathcal{S}_{\text{STAMP}}, \mathcal{E}}$. Therefore, in **Case 1** the view of \mathcal{A} and \mathcal{E} are indistinguishable in the real and the simulated world.

Putting it all together, we have that $\mathcal{H}_0 \approx \mathcal{H}_1 \approx \mathcal{H}_2 \approx \mathcal{H}_3 = \mathcal{S}_{\text{STAMP}}$. \square

Notice that as discussed in [§4.4](#), the above proof works identically for $\text{MatMulBatchNormReLU}$ and MatMulMaxPoolReLU since only the plaintext computations after subtracting the masks are different.

Next, we will prove the [Theorem 3](#). We provide the complete proof for case 1 (where P_1 is corrupted) due to the space limit, and the proof of the other two cases is similar to what we did previously.

$\mathcal{F}_{\text{Softmax}}$

- 1) Upon receiving inputs $(\mathbf{x}_{3,1}, \mathbf{x}_{1,1}), (\mathbf{x}_{1,2}, \mathbf{x}_{2,2}), (\mathbf{x}_{2,3}, \mathbf{x}_{3,3})$ from P_1, P_2, P_3 respectively, check if $\mathbf{x}_{j,j} = \mathbf{x}_{j,j+1}$ for $j = 1, 2, 3$. If not, notify abort. Otherwise, compute $\mathbf{x} = \mathbf{x}_{1,1} + \mathbf{x}_{2,2} + \mathbf{x}_{3,3}$, $\mathbf{z} = \lfloor \exp(\mathbf{x}) \gg \text{fp} \rfloor \ll \text{fp}$. Then, send a signal ($\text{Softmax}, \mathbf{x}_{i-1,i}, \mathbf{x}_{i,i}, n, L, i$) to $\mathcal{S}_{\text{STAMP}}$ that includes the inputs of P_i , the size of inputs of P_{i+1} and P_{i-1} , and the index i of the corrupted party.
 - 2) Upon receiving ($\text{Softmaxend}, i, \mathbf{z}_{i-1}, \mathbf{z}_i$) from $\mathcal{S}_{\text{STAMP}}$, let $\mathbf{z}_{i+1} = \mathbf{z} - \mathbf{z}_{i-1} - \mathbf{z}_i$. Return $(\mathbf{z}_i, \mathbf{z}_{i+1})$ to the P_i for $i = 1, 2, 3$.
-

Figure 9: Ideal functionality for Π_{Softmax} .

$\mathcal{F}_{\text{SoftmaxLTH}}$

Upon receiving signal with inputs \mathbf{x}' , masks \mathbf{m} and party index i , compute the following:

- 1) $\mathbf{x} = \mathbf{x}' - \mathbf{m}$, $\mathbf{a} = \lfloor \exp(\mathbf{x}) \gg \text{fp} \rfloor \ll \text{fp}$.
 - 2) Generate random $\mathbf{z}_1, \mathbf{z}_2, \mathbf{z}_3$ such that $\mathbf{z}_1 + \mathbf{z}_2 + \mathbf{z}_3 = \mathbf{z}$. Returns $(\mathbf{z}_i, \mathbf{z}_{i+1})$ to P_i (as mentioned in notation, for party index $i + 1$ means the next party).
-

Figure 10: Ideal functionality for the LTH part of Π_{Softmax} .

Proof for [Theorem 3](#). We prove [Theorem 3](#) by constructing a simulator and a series of hybrid games similar to the Proof of [Theorem 1](#), with \mathcal{E} providing inputs to parties.

Case 1: P_1 is corrupted ($i = 1$) and P_2, P_3 are honest.

The Simulator. $\mathcal{S}_{\text{STAMP}}$ simulates the following interactions on receiving the signal from $\mathcal{F}_{\text{ReLU}}$:

Communication Type	Framework	ReLU	MaxPool	Batch/LayerNorm	Softmax
Network comm. rounds	Falcon+	10	$12(w^2 - 1)$	335	-
	AriaNN	2	3	9	-
	STAMP	2	2	2	2
Network comm. data	Falcon+	$16n$	$20m^2 + 4w^2$	$224n$	-
	AriaNN	$12n$	$((m-w)/s + 1)^2(w^4 + 1)$	$72n$	-
	STAMP	$5n$	$\frac{2}{3}(2n + 2w^2 + 5((m-w)/s + 1)^2)$	$4n$	$\frac{20}{3}n$
LTH comm.	STAMP	$\frac{25}{3}n$	$\frac{1}{3}(8m^2 + 8w^2 + 15((m-w)/s + 1)^2)$	$\frac{16}{3}n$	$\frac{44}{3}n$

Table 7: Analytical cost analysis of the network communication rounds and amount (in Bytes) under the semi-honest setting, and the local bus communication with the LEE. Here, $n = m \times m$ is the input size, s is the stride, and the filter size is set to $w \times w$.

- Upon receiving $(\text{Softmax}, 1, \mathbf{x}_{3,1}, \mathbf{x}_{1,1}, n, L)$ from $\mathcal{F}_{\text{Softmax}}$, $\mathcal{S}_{\text{STAMP}}$ generates a random $\hat{\mathbf{x}}_2$, and use $(\mathbf{x}_{1,1}, \hat{\mathbf{x}}_2)$ and $(\hat{\mathbf{x}}_2, \mathbf{x}_{3,1})$ as dummy inputs for P_2 and P_3 , respectively.
- $\mathcal{S}_{\text{STAMP}}$ acts as $\mathcal{F}_{\text{GenMask}}$ to generate random masks $\alpha_j \in \mathbb{Z}_{2^{52}}$ and $\beta_j \in \mathbb{Z}_{2^{32}}$ for $j = 1, \dots, n$ for P_1 , then computes $\bar{r} = \exp((\mathbf{x}_{3,1})_j \gg \text{fp})$ for $j = 1, \dots, n$. Let $\bar{r} = \exp((\mathbf{x}_{3,1})_j \gg \text{fp}) = 2^{q_j} \cdot (m_j \gg 52)$ as noted. $\mathcal{S}_{\text{STAMP}}$ computes $\{m_j^* = (m_j + \alpha_j)_{2^{52}}, q_j^* = (q_j + \beta_j)_{2^{32}}\}$ for $i = 1, \dots, n$ as P_1 sending to P_2 . $\mathcal{S}_{\text{STAMP}}$ repeat above for P_3 , replacing $\mathbf{x}_{3,1}$ with $\mathbf{x}_{3,3}$; $\mathcal{S}_{\text{STAMP}}$ again repeat above as P_2 and P_3 , each replacing $\mathbf{x}_{3,1}$ with $\mathbf{x}_{2,2}$ and $\mathbf{x}_{2,3}$, with Π_{LTH} generating (α', β') , and get $\{m_j^*, q_j^*\}$ respectively. $\{m_j^*, q_j^*\}$ are for P_2 provided by P_1 and P_2 , and $\{m_j^*, q_j^*\}$ are for P_1 provided by P_2 and P_3 .
- $\mathcal{S}_{\text{STAMP}}$ compare the received copies as P_2 and P_1 , and signal abort to $\mathcal{F}_{\text{Softmax}}$ if an inconsistency is found. $\mathcal{S}_{\text{STAMP}}$ computes as P_2 : $2^{(q_2)_j} \cdot (m_2)_j := \exp(((\mathbf{x}_{2,2})_j + (\mathbf{x}_{1,2})_j) \gg \text{fp})$ for $j = 1, \dots, n$. $\mathcal{S}_{\text{STAMP}}$ computes as P_1 : $2^{(q_1)_j} \cdot (m_1)_j := \exp(((\mathbf{x}_{1,1})_j + (\mathbf{x}_{3,1})_j) \gg \text{fp})$ for $j = 1, \dots, n$.
- $\mathcal{S}_{\text{STAMP}}$ acts as $\mathcal{F}_{\text{LTHSoftmax}}$ with P_2 's input $\{\mathbf{q}^* + \hat{\mathbf{q}}_2, \mathbf{m}^*, \hat{\mathbf{m}}_2\}$ to H_1 , to (re)generate (α, β) , then locally compute \mathbf{y} as in step 4) $\mathcal{S}_{\text{STAMP}}$ then generate $\mathbf{m}_1 + \mathbf{m}_2 + \mathbf{m}_3 = \mathbf{0}$ and $(\mathbf{m}_1 + \mathbf{y}, \mathbf{m}_2)$ as $(\mathbf{y}_{1,2}, \mathbf{y}_{1,2})$ for P_2 . $\mathcal{S}_{\text{STAMP}}$ acts as $\mathcal{F}_{\text{LTHSoftmax}}$ with P_1 's input $\{\mathbf{q}^* + \hat{\mathbf{q}}_1, \mathbf{m}^*, \hat{\mathbf{m}}_1\}$ to H_1 , to (re)generate (α', β') , then locally compute \mathbf{y} as in step 4). $\mathcal{S}_{\text{STAMP}}$ then generate $\mathbf{m}_1 + \mathbf{m}_2 + \mathbf{m}_3 = \mathbf{0}$ and $(\mathbf{m}_3, \mathbf{y} + \mathbf{m}_1)$ as $(\mathbf{y}_{3,1}, \mathbf{y}_{1,1})$ for P_1 . $\mathcal{S}_{\text{STAMP}}$ send
- $\mathcal{S}_{\text{STAMP}}$ checks $\mathcal{S}_{\text{STAMP}}$ compare $\mathbf{y}_{1,1} = \mathbf{y}_{1,2}$ as P_1 and P_2 ; $\mathbf{y}_{2,2} = \mathbf{y}_{2,3}$, $\mathbf{y}_{3,3} = \mathbf{y}_{3,1}$ as P_3 . Signal abort to $\mathcal{F}_{\text{Softmax}}$ if an inconsistency is found. If no abort is signaled, $\mathcal{S}_{\text{STAMP}}$ signals $(\text{Softmaxend}, 1, \mathbf{y}_{3,1}, \mathbf{y}_{1,1})$ to $\mathcal{F}_{\text{Softmax}}$.

Indistinguishability. We prove the indistinguishability argument by constructing a sequence of hybrid games as follows.

Hybrid \mathcal{H}_0 : This is the real protocol execution.

Hybrid \mathcal{H}_1 : \mathcal{H}_1 is the same as \mathcal{H}_0 , except that we replace $\Pi_{\text{LTH.GenMask}}$ with simulated $\mathcal{F}_{\text{GenMask}}$ that outputs random (α, β) and (α', β') for both step 1) and 3).

Hybrid \mathcal{H}_2 : \mathcal{H}_2 is the same as \mathcal{H}_1 , except that we replace step 4) with the simulated $\mathcal{F}_{\text{LTHSoftmax}}$.

Proofs of \mathcal{H}_0 and \mathcal{H}_1 , \mathcal{H}_1 and \mathcal{H}_2 being computationally indistinguishable are similar to the proof of [Theorem 1](#), with the actual random masks replaced by (α, β) and (α', β') .

Hybrid \mathcal{H}_3 : \mathcal{H}_3 is the same as \mathcal{H}_2 , except that P_2, P_3 use dummy inputs for interaction, instead of the ones provided by the environment. In this hybrid, we introduce an ideal functionality $\mathcal{F}_{\text{Softmax}}$ that takes the environments' actual inputs and returns the corresponding outputs.

We claim that \mathcal{H}_2 and \mathcal{H}_3 are indistinguishable. Since the corrupted party is P_1 , $\mathcal{S}_{\text{STAMP}}$ knows $\mathbf{x}_{3,1} = \mathbf{x}_{3,3}$, $\mathbf{x}_{1,1} = \mathbf{x}_{1,2}$. The dummy inputs would be $\mathbf{x}_{2,2} = \mathbf{x}_{2,3}$ (represented by $\hat{\mathbf{x}}_2$ in $\mathcal{S}_{\text{STAMP}}$). The computation result sent to P_1 by P_3 in step 1) used the dummy inputs, and $\{m_j^* = (m_j + \alpha'_j)_{2^{52}}, q_j^* = (q_j + \beta'_j)_{2^{32}}\}$ for $i = 1, \dots, n$ are uniformly random since (α', β') are random. Therefore the views of adversary in step 1) are not distinguishable in both hybrids, and its views of step 3) and 4) are also not distinguishable in both hybrids due the uniformly masked output. Therefore, \mathcal{H}_2 and \mathcal{H}_3 are indistinguishable.

The adversary's view of \mathcal{H}_3 is identical to $\text{EXEC}_{\mathcal{F}, \mathcal{S}_{\text{STAMP}}, \mathcal{E}}$. Therefore, in **Case 1** the view of \mathcal{A} and \mathcal{E} are indistinguishable in the real and the simulated world.

Putting it all together, we have that $\mathcal{H}_0 \approx \mathcal{H}_1 \approx \mathcal{H}_2 \approx \mathcal{H}_3 = \mathcal{S}_{\text{STAMP}}$. □

Appendix C. Additional Analysis

The cost analysis is shown in [Table 7](#). The byte size of the finite field is chosen to be 4 and we count the exponent and the mantissa part in [Protocol 6](#) as 4 and 8 bytes. AriaNN [67] results are from their articles. We see significant improvements in inter-party communication rounds compared to Falcon, and significant theoretical reduction in the amount of communication data compared to both Falcon and AriaNN.

The actual speedup of a particular neural network depends on its structure including the ratio between linear and non-linear operations, the order of linear/non-linear operations/layers (which determines if protocols like [Protocol 5](#) can be applied), the input dimensions, etc. The

communication setting and the computational power also matter. We discuss the performance in §5.

Appendix D. Pure TEE Solution

Network	Network-A	Network-B	Network-C	LeNet
STAMP	0.0737	0.1172	0.6809	0.9693
Pure SGX	0.4616	0.4612	0.4612	0.5067
Network	AlexNet	Transformer	VGG16	ResNet18
STAMP	1.5644	0.5130	26.558	309.71
Pure SGX	5.0308	-	-	8.1562

Table 8: STAMP or SGX execution time. We use the semi-honesty LAN/GPU results of STAMP for a comparison.

We put the data obtained for the pure TEE solution here in Table 8. Some data cannot be obtained due to the limit of the size of the SGX enclave.